NEAR-INFRARED EMISSION SPECTROSCOPY OF EXPLOSIVE BREAKOUT

BY

AUSTIN HERMAN

THESIS

Submitted in partial fulfillment of the requirements
for the degree of Master of Science in Mechanical Engineering
in the Graduate College of the
University of Illinois at Urbana-Champaign, 2017

Urbana, Illinois

Adviser:

Professor Nick G. Glumac

ABSTRACT

The aim of this study was to explore the early time breakout in the near infrared spectrum of various high explosives. Explosives tested include RDX, Composition B, HMX, and PETN, along with RP1 and RP80 detonators in air and nitrogen environments. The first 20 microseconds after detonation were examined using a combination of a rotating filter disk and shutter to gate the exposure after the detonation. The spectral range covered in this study included from approximately 880 to 1660 nm. Various spectrometer systems were used that resulted in two ranges of resolution. Notable spectral features were compared to previous work, and emission spectrum of diatomic and atomic sources were investigated. Simulations of possible molecular and atomic species were studied using the Specair software. The result of this study led to the positive identification of several key emitters, while others remain unidentified.

To my loving parents

ACKNOWLEDGEMENTS

In my effort to complete this thesis in partial fulfillment of the requirements for the degree of Master of Science in Mechanical Engineering there are several people I would like to acknowledge that have assisted me in my journey. First, I would like to thank my family, specifically my parents Greg and Mary, to whom I have dedicated this thesis. Throughout my entire education, I have always had their constant love and support. It has been their belief in my abilities that has made this journey all the easier.

Second, I would like to thank several fellow members of my research group. I would like to specifically thank Chris Murzyn. I first began working as an undergraduate researcher in this group. Once I began my graduate career, there has been many a times that he has assisted me with working through problems. I would also like to thank Jesse Evans and Kevin Schafer who have been a constant source of moral support at our weekly evening meetings. Each one has been a dear friend and source of happiness. Lastly, I would like to thank my advisor Dr. Nick Glumac and Dr. Herman Krier. Dr. Glumac has allowed me to earn my Master's degree by conducting research under his guidance and Dr. Herman Krier who has been kind enough to review this thesis.

TABLE OF CONTENTS

LIST OF FIGURES

LIST OF TABLES

CHAPTER 1: INTRODUCTION

1.1. Scope

The aim of this study was to explore the early time breakout in the near infrared spectrum of various high explosives. Explosives tested include RDX, Composition B, HMX, and PETN, along with RP1 and RP80 detonators. The first 20 microseconds after detonation were examined using a combination of a rotating filter disk and shutter to gate the exposure after the detonation. The maximum spectral range covered from 880 to 1660 nm. Various spectrometer systems were used with two ranges of resolution: a "low" resolution (~3-4 nm) range and a "high" resolution (~0.5 nm) range. Notable features observed in the low resolution tests were repeated with higher resolution spectrometer systems. A comparison of both low and high resolution tests was conducted in air and nitrogen environments resulting in a total of 11 tests. Notable spectral features were compared to previous studies conducted and the emission spectrum of likely diatomic and atomic sources were investigated.

1.2. Motivation

A relatively new and unexplored topic of interest for combustion research in recent years has been early time-resolved emission spectroscopic measurements during high explosive detonation. Up until this point, there has not been significant work completed on this topic in the near infrared spectrum. Only a handful of experiments appear to be completed in any part of the electromagnetic spectrum for any high explosive. One objective of this study is to collect early time spectra (1-20 μs) of several high explosives that have not been studied before, at least to the

best of the author's knowledge. A second objective is to repeat similar tests for explosives that have been previously completed in the hope to replicate the results of those studies.

The topic of interest comes with the usual difficulties involved with combustion studies, especially high explosives testing. Measurements prove to be difficult with the sub micro-second time scales and extreme pressure and temperature environments involved in these types of experiments. Some measuring techniques, besides optical means, have response times longer than the time scales of interest and also do not survive the destructive nature of such reactions. Other optical techniques, such as pyrometry, are often easily implemented, but quantitative interpretation is often problematic. The reasons spectroscopic techniques are often chosen over other optical techniques is the fact that spectrally resolved emission measurements offer the possibility to identify individual species and also to infer electronic temperatures, even though it usually is a path averaged technique.

The benefits from these types of experiments often give insight to the detailed chemistry and energy release rates of high explosives. By using time-resolved emission spectroscopy methods to characterize the complex chemical dynamics, one may be able to shed light onto otherwise unknown short lived species and temperature variations that occur following the detonation of an explosive charge. These techniques could further allow for species concentration measurements.

1.3. Limitations

As previously stated, the aim of this study was to explore the early time breakout in the near infrared spectrum of various high explosives. With this goal in mind this study has several limitations to its scope. First, this study is limited to covering the range of 880 – 1660 nm with a resolution of approximately 3-4 nm. Several higher resolution tests were conducted, but these were still limited to this spectral range. Second, each test conducted covered only the first 20 microseconds due to the equipment used. Previous studies did record a longer total time with similar time segments due to the capabilities of equipment used. Lastly, each test was only performed once. These limitations will in hope be resolved by future work stated in recommendations section.

1.4. Overview

This document is separated into several chapters that contribute to various aspects. Chapter 2 begins by introducing a brief description of high explosives in general and those explosives specifically used in this study. The chapter continues with previous studies that have been conducted. Earlier works include near infrared air shock work. This work should replicate similar results seen in high explosive detonations. The chapter ends with a review of previous research covering emission spectroscopy of explosives near breakout.

Chapter 3 describes the experimental methods used. The experimental setup along with the equipment used is covered. The methodology used for triggering and gating used to achieve the first 20 microseconds after detonation is discussed. In addition, outputs for data collection used

and the specific test matrix are covered. Lastly, the data processing of the raw data collected throughout the experiments is explained.

Chapter 4 presents the results for the various tests described. Data of the various spectra of the high explosives/detonators in the various environments in low and high resolution is presented. Chapter 5 includes the discussion over the experimental results. It works to identify the key emitters of the notable features in the spectra and presents the information that is known. Key features are compared to simulated spectra using Specair software. Chapter 6 presents conclusions with a summary of the research presented and recommendations for further work.

CHAPTER 2: LITERATURE REVIEW

2.1. High explosives

Explosives have a long history with its beginning originating with the first real record of gunpowder being discovered in the 13th century. Gunpowder is a mixture of potassium nitrate, charcoal and sulfur very intimately ground together. Roger Bacon brought the knowledge of gunpowder back to Europe in 1251, but kept it a secret to himself in a cypher. It was rediscovered in the fourteenth century by Berthold Schwarz who is often credited to bringing the knowledge to Germany where it earned the name *Schwarzpulver*, which translates into English as black powder. Several centuries later, two notable achievements occurred in the field with the discovery of nitroglycerine by Ascanio Sobrero in 1847 and TNT by Julius Wilbrand in 1863. Nitroglycerine became the first with commercial importance due to the effort of Alfred Nobel who developed a safe method for its production. Nobel's other notable achievements include the modern mercury fulminate detonator, dynamite, and blasting gelatine [1].

"Energetic materials" is a broad term that generally characterizes a substance that does not need additional oxidizer for temperature sensitive reactions that are highly exothermic. Explosives are one of three subcategories under energetic materials with the other two being propellants and pyrotechnics. Explosives are often described as substances when subjected to heat, percussion, detonation, or catalysis, release a large amount of heat and pressure by a very rapid self-sustaining exothermic decomposition reaction [2].

Explosives may be subcategorized into high or detonating explosives and low or deflagrating explosives with the former being characterized by higher rates of reaction on the order of microseconds, higher pressures (50,000-4,000,000 psi), and being easier to detonate while the latter is characterized by slower rates of reaction on the order of milliseconds, lower pressures (up to about 50,000 psi), and being more difficult to detonate [3]. High explosives may be further subdivided into primary, secondary, and tertiary explosives.

Primary high explosives are very sensitive materials that are easily ignited by the application of fire, spark, impact, or friction. Primary explosives detonate by burning and therefore the most important property of a primary explosive its ability to undergo a fast deflagration-to-detonation transition (DDT). This quality is also why they are dangerous to handle and are often used in comparatively small quantities in primers, detonators, or percussion caps. Some examples of primary explosives include lead azide, mercury fulminate, silver azide [2].

Secondary explosives are less sensitive compared to primary explosives and detonate because of shock waves. They are usually detonated in larger quantities by using a primary explosive as a detonator. Secondary explosives are sometimes coupled with a booster, which is a sensitive secondary high explosive that reinforces the detonation wave from the detonator and thereby delivers a more powerful detonation wave to the main secondary explosive [2-3]. The various high explosives used in this study fall under this category. A primary reason these explosives were chosen is due to the safety of their insensitive nature and reliable detonation in relative quantities. As previously mentioned, the high explosives in this study include: 1) RDX, 2) Composition B, 3) HMX, and 4) PETN.

Research Department Explosive (RDX) is a monomolecular secondary high explosive that was discovered in 1899 by Georg Friedrich Henning. It is also known by other names, such as cyclonite in the US, hexogen in Germany, and T_4 in Italy. Its chemical name is cyclotrimethylene trinitramine or 1,3,5-trinitrohexahydro-*sym*-triazine and its chemical formula is $(CH_2)_3(NNO_2)_3$. It is a white crystalline solid with melting point at 202–204 °C and density 1.82 gcm^{-3}. RDX has high chemical stability and high explosive power. RDX has a detonation velocity of 8600 ms^{-1} and a detonation pressure of 33.8 GPa. During World War II, RDX was developed for filling hand and anti-tank grenades, but was widely used as a base for many common mixtures, such as Composition B that will be discussed next [1-2].

Composition B is a composite secondary high explosive usually consisting of 39% TNT, 60% RDX, and 1% wax by weight with a density of 1.71 gcm^{-3}. It has a detonation velocity of 8050 ms^{-1} and a detonation pressure of 28.1 GPa. Composition B was also widely used for military applications beginning in World War 2 until the 1950's. The Fat Man atomic bomb dropped on Nagasaki used Composition B as a high VOD explosive [2].

High Melting Explosive or Her Majesty's Explosive (HMX) is a monomolecular secondary high explosive that was discovered in 1941 by Bachmann. It is also known as Octogen. Its chemical name is cyclotetramethylene tetranitramine or 1,3,5,7-tetranitro-1,3,5,7-tetraazacyclooctane and its chemical formula is $(CH_2)_4(NNO_2)_4$. HMX is a white crystalline substance and exists in four polymorphic modifications with the β form being most stable and least sensitive. It has a density

of 1.91 gcm^{-3} and a melting point at 291°C. HMX is reported to be the fastest high explosive with a detonation velocity of 9100 ms^{-1} and a detonation pressure of 39.5 GPa. HMX is considered a superior explosive than RDX because of its higher chemical stability, higher density, higher velocity of detonation. HMX is used in mixtures with TNT or bonded with plastics [2].

Pentaerythritol tetranitrate (PETN) is a monomolecular secondary high explosive that was discovered in 1895 by the explosives manufacturer Rheinisch-Westfälische Sprengstoff. Its chemical formula is $C(CH_2)_4(ONO_2)_4$ and is a white crystalline solid with a density of 1.77 gcm^{-3} and a melting point at 140°C. PETN has a detonation velocity of 8000 ms^{-1} and a detonation pressure of 32.0 GPa. PETN is often considered a benchmark explosive, with explosives that are more sensitive than PETN being classified as primary explosives. Similar to RDX, PETN was developed for filling hand and anti-tank grenades during World War II. It has been used extensively with TNT under the name Pentolite for loading of small caliber projectiles and grenades [1-2].

The last category of high explosives are tertiary explosives. These are often oxidizers that are detonated in large quantities. It is difficult to detonate tertiary explosives by fire, impact or friction. Tertiary explosives are so insensitive to shock detonation that that they cannot reliably be detonated by practical quantities of primary explosives. Instead, secondary explosives are required as an intermediate explosive booster. Some common tertiary explosives include ammonium nitrate, ammonium perchlorate, and mononitrotoluene [2].

2.2. Near infrared air and nitrogen shock work

The first works most similar to the current study would have been achieved by near infrared air shock work with a majority of this work was conducted in the 1960's and 1970's. These types of studies would replicate temperatures and pressures via shock waves that would resemble high explosives detonation environments.

Firstly in 1962 Wurster *et. al* reported work on nitric oxide bands near 1 micron in shock-heated air [4]. Wurster also discussed similar work in a paper from 1963 [5]. The infrared emission spectrum from pure nitrogen, oxygen, and air was studied between 800-1400nm. The study conclusively demonstrated the structure in the region requires the presence of both N2 and O2 by comparison of air, nitrogen, and oxygen environment. The radiation intensity was shown to be proportional to the concentration of NO present in the experiments at 1.04 microns. Further, the temperature dependence was in general agreement with that expected from the excited electronic states of NO at 1.04 micron [4].

However, Wray and Connolly believed there may be reason to doubt the NO assignment at 1.04 microns [6]. The lack of correct pressure scaling and the anomalously high apparent f- numbers obtained from their data gave reason to question this assignment. With these questions raised, Wurster and Marrone decided to re-examine the previous work with another set of experiments to resolve these issues [7-8]. As a result of this work Wurster and Marrone believed they confirmed their previous results that NO is a dominant source in the infrared, specifically at wavelengths 1.03, 1.13, and 1.21 microns.

Wray continued with similar work, but instead of shock tubes he used a continuously running 1 atm constricted arc jet to prepare equilibrium air and nitrogen at temperatures between 3500 and 5800°K [9]. Spectrum taken in air showed several atomic lines identified as belonging to O and N in addition to N_2 (1+) bands. In nitrogen, similar spectra are observed except for the absence of the atomic O lines. Once again, there was extra radiation observed in the air spectrum that cannot be completely accounted by the N_2 (1+) bands. Another study of electric discharges in air was completed by Benesch and Saum in 1971 [10]. This study also showed many atomic O and N lines and a molecular band belonging to the NO electronic band system $C^2\Pi \rightarrow A^2\Sigma^+$ in the area of interest.

2.3. Emission spectroscopy of high explosives

The majority of related work on early high explosive detonation has been completed in the UV-VIS regions. Further many of the studies conducted have been with aluminized explosives. In these regions, many of the spectral features observed are dominated by Al, AlO, and other atomic impurities. In 2005, work by Weiser and Eisenreich involved fast emission spectroscopy for a better understanding of pyrotechnic combustion behavior [11]. Part of their study involved a medium resolved UV/VIS spectrum from 200 – 500 nm (~1 nm wavelength resolution) of a 95/5 RDX/Estane flame at a pressure of 0.5 MPa in nitrogen atmosphere. Emission bands of the decomposition products OH, CN and NH were observable [11].

Carney *et. al* in 2006 conducted research into time-resolved optical measurements of the post-detonation combustion of aluminized PBXN-113 N113, which is a mixture of the traditional explosive HMX octahydro-1,3,5,7-tetranitro-1,3,5,7-teti-azocine, aluminum, and a polymer binder. Spectra from 360 – 560 nm of 11 μs, 19 μs, and 38 μs delay after the detonator trigger were examined showing Al and AlO features [12].

Work by Lewis *et. al* has involved spectroscopic studies of RDX in 2009 and 2012 [13-14]. In 2009 charges of either RDX or RDX doped with a 1 wt. % of barium nitrate were prepared. Emission spectra of the post detonation fireball was collected from 460 – 800 nm. The emission spectra show several broad emissions as well as sharp lines, but Lewis and Rumchik did not attempt to identify more than the atomic features that were later used to estimate the temperature of the fireball to characterize the energy release associated with the explosion [13].

In 2012, Lewis *et. al* continued similar work using both non-aluminized and aluminized RDX charges containing 20 wt. % of either 30-70 nm or 16-26 μm Al particles. Time-resolved early time detonation emission spectra was collected from time 0 to 120-150 μs. Similar results from 2009 study was found for the non-aluminized RDX charges doped and undoped with $Ba(NO_3)_2$. Clear signs of Al atomic emission peaks, an AlO vibronic band, and a broadband emission that is typical of aluminum combustion were observed in the aluminized RDX charges [14].

The closest research to the present study was performed by Koch *et. al* in 2010, where temporally and near infrared spectrally-resolved emission measurements during post detonation combustion of pentaerythritol tetranitrate (PETN) charges were made [15]. Charges were either

composed of pure PETN or 90 wt. % PETN with 10 wt. % of four different microparticles. The four microparticle configurations were: (1) 1 μm diameter silver, (2) 5 μm silver-coated aluminum, (3) a mix of 5 wt. % 5 μm diameter silver and 5 wt. % Valimet H-5 aluminum, and (4) a mix of 5 wt. % 5 μm silver iodate and 5 wt. % H-5 aluminum. In this study a NIR emission spectrum from 750 to 1500 nm following detonation of pure PETN in atmospheric air, shortly after breakout (0 – 21 μs) is recorded. Koch *et. al*, to the best of their knowledge, believe this work represents the first early-time NIR emission measurement of PETN exploding in ambient air [15].

They suggest several of the peaks may be potassium may be emitting near 766, 770, and 1177 nm, and sodium near 819 and 1128 nm. These are most likely impurities in the PETN. Other peaks they theorize might be high lying atomic oxygen or nitrogen lines at 777, 844, 926, and 1128 nm for atomic O and 865 and 938 nm for atomic N. There are also other features that do not appear to coincide any known impurities or air products [15]. The features between 1000 – 1300 nm closely resemble some of the results from this work and will be discussed in later chapters.

In 2012 Glumac examined the explosive breakout of PBX-9407 into air using time-resolved optical spectroscopy in the UV-VIS region [16]. For the 200 – 550 nm range, spectral emission from Ca I, Ca II, OH, and CN were easily identified. From the visible region, spectra were taken from 400 – 650 nm with 1 μs exposure times. These spectra show several interesting features that all appear until 15 μs. Atomic lines appear in the first 3 μs and then mostly fade leaving several

prominent band structures around 535, 555, 605, and 620 nm. These features resemble molecular bands or closely grouped clusters of broadened atomic lines [16].

CHAPTER 3: EXPERIMENTAL METHODS

3.1. Experimental Setup

The basic layout for the experiments conducted in this study follow the setup shown in Figure 3.1. There were several variations to this setup. In general, one of two custom blast chambers built by Professor Glumac inside the Mechanical Engineering Lab (MEL) were used to contain the various explosives. Blast chamber #1 was cylindrical with an approximate inner diameter of 150 mm and internal length of 300 mm. Blast chamber #2 was a smaller cylindrical chamber with an approximate inner diameter of 50 mm and internal length of 150 mm. Photographs of both blast chambers are shown below in Figure 3.2.

Optical access was allowed through each blast chamber and collimated light was collected from f/4 lens system. Both lenses were 50 mm diameter fused silica plano-convex lens with 100 mm focal length. The upstream focus was on the end of the charge inside the blast chamber, and the downstream focus was on the entrance slit of one of two spectrographs. Between the two lenses were a Thorlabs SH05 shutter and a custom rotating filter disk used for gating. The rotating disk had a slit approximately 2 mm by 20 mm in size and was attached to a MFA Como Drill 919D series single ratio metal gearbox.

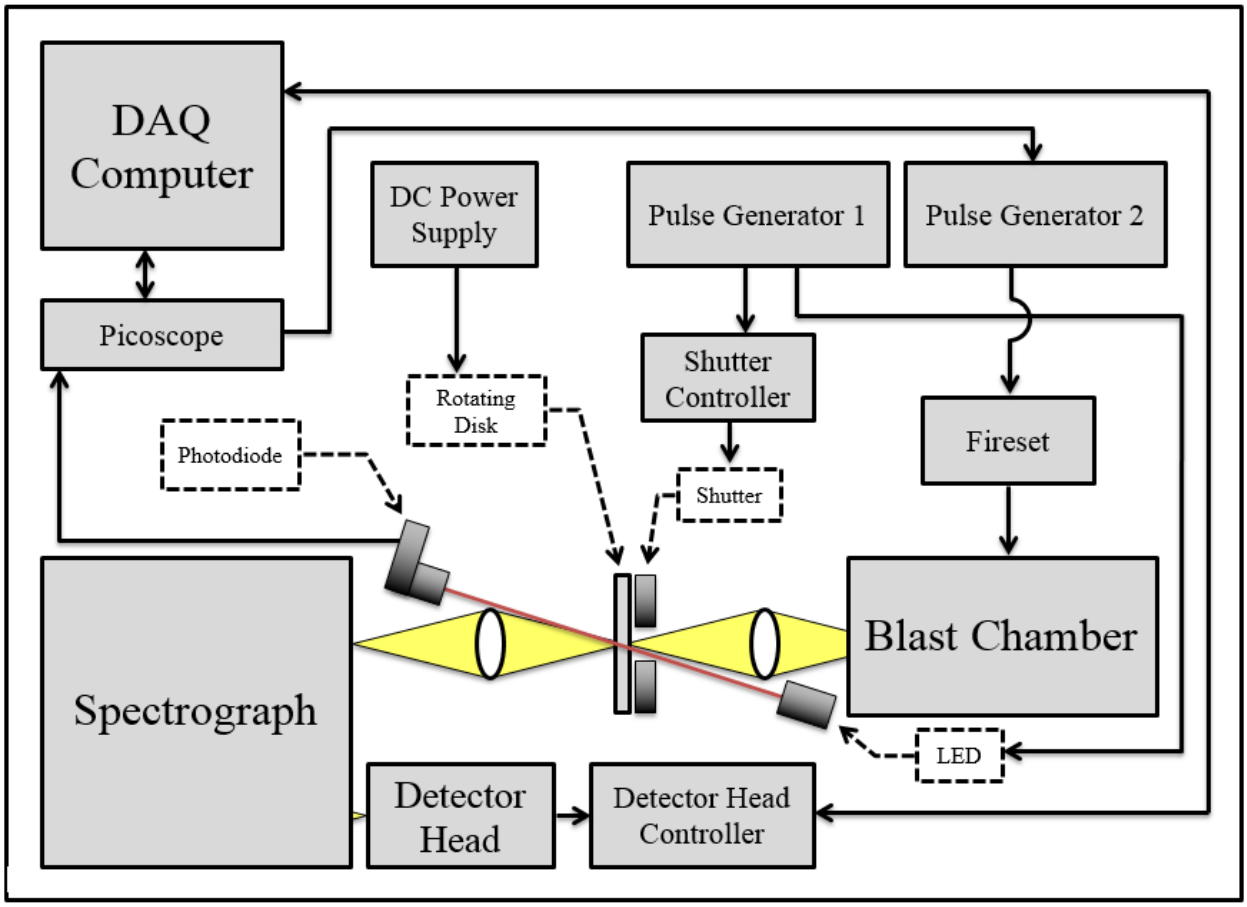

Figure 3.1: Experimental setup diagram during testing

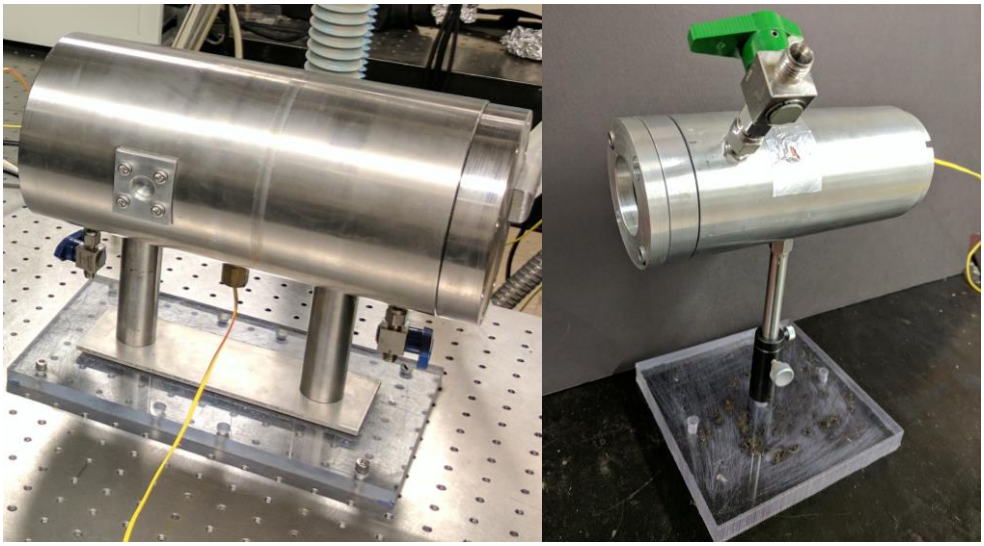

Figure 3.2: Custom blast chamber #1 (left) and custom blast chamber #2 (right)

The variation of the general setup includes several combinations of blast chamber, spectrograph, grating, and detector head that is described in the following 4 cases.

Case 1: Custom blast chamber #1 was used to contain the charges. A conventional TRIAX 190 spectrograph having a deviation angle of 25°, focal length 190 mm, and entrance slit width of 50 microns was used. Along with the spectrograph a 75 gr/mm ruled diffraction grating blazed at 3 microns provided a resolution of approximately 4 nm. This spectrograph was coupled with a Hamamatsu InGaAs linear image sensor (Model: G9214-512S). The sensor area was 512 by 1 pixels with a pixel height/width of 25 microns. The sensor was controlled using a multichannel detector head (Model: C8061-01) and multichannel detector head controller (Model: C7557). A photograph of this case is presented in Figure 3.3.

Case 2: All was the same as Case 1, except a 600 gr/mm ruled diffraction grating blazed at 1 micron was used. This provided approximately 0.5 nm resolution.

Case 3: All was the same as Case 1, except a conventional SPEX 270 spectrograph having a deviation angle of 17° and focal length of 270 mm was utilized. With the entrance slit width set to 50 microns once again this system provided approximately 3 nm resolution.

Case 4: Custom blast chamber #2 was used to contain the charges with the same conventional SPEX 270 spectrograph as Case 3. Along with the spectrograph a 600 gr/mm ruled diffraction grating blazed at 1 micron provided a resolution of approximately 0.5 nm. This spectrograph was coupled with a Hamamatsu CCD image sensor (Model: S7031-1006S). The sensor area was 1044 by 64 pixels with a pixel height/width of 24 microns. The sensor was controlled using multichannel detector head (Model: C7041) and multichannel detector head controller (Model: C7557-01).

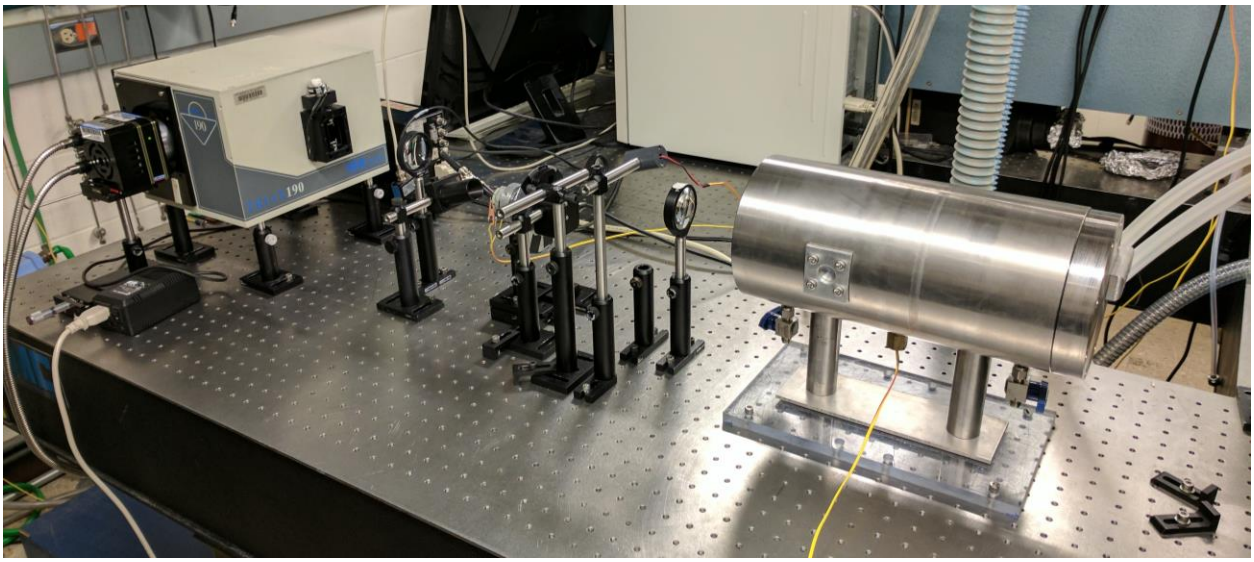

Figure 3.3: Case 1 experimental setup

3.2. Data Collection

The only output from each experiment was a single spectrum collected via the Hamamatsu multichannel detector heads for each variation of the experimental setup previously described.

The detectors started taking a series of spectra for several seconds each with 50 ms programmed exposure time. An exposure time of the first 20 μs after detonation was achieved via the gating described in the following section.

3.3. Gating and triggering sequence

The goal for this research was to obtain spectra of the first 20 μs after detonation for each of the experiments that will be described in the following section. The detectors used have a minimum exposure time limit on the order of a few milliseconds. A rotating filter disk and Thorlabs shutter was implemented to compensate for the detectors limitations. A closer view of the gating system can be seen in Figure 3.4 below. The rotating filter disk was controlled via a DC voltage power supply and set to rotate at approximately 10,000 rpm. At this speed the slit of the rotating disk would complete one rotation every 6 ms. The Thorlabs shutter could fully close in approximately 15 ms.

To prepare the timing before tests, photodiodes were placed inside (Model: PDA36A) and outside (Model: DET36A) the spectrograph along with LEDs. Both photodiodes possessed rapid response times on the order of several nanoseconds. One LED would be placed in the location of the blast chamber and the other LED remained in the location as shown in Figure 3.4. The LED pointing to the photodiode outside the spectrometer was powered by a Quantum Composers pulse generator series 9520 (Labeled pulse generator 1 in Figure 3.1). Timing was monitored and adjusted using a Picoscope 3203D series to allow only one rotation of the filter disk by using the

LED/photodiode outside the spectrograph as a triggering signal. Overall, the triggering sequence went as follows:

1) Detectors were manually triggered to begin taking a series of spectra over a span of several seconds. A second after spectra was starting to collect pulse generator 1 would also be manually triggered.

2) Pulse generator 1 would simultaneously signal the Thorlabs shutter to close and power the trigger LED with a delay.

3) Once the photodiode outside the spectrograph detects the signal from the trigger LED, the Picoscope would be send a delayed signal to a Tenma TGP110 Pulse Generator (Labeled pulse generator 2), which would then immediately trigger the fireset to detonate the charge.

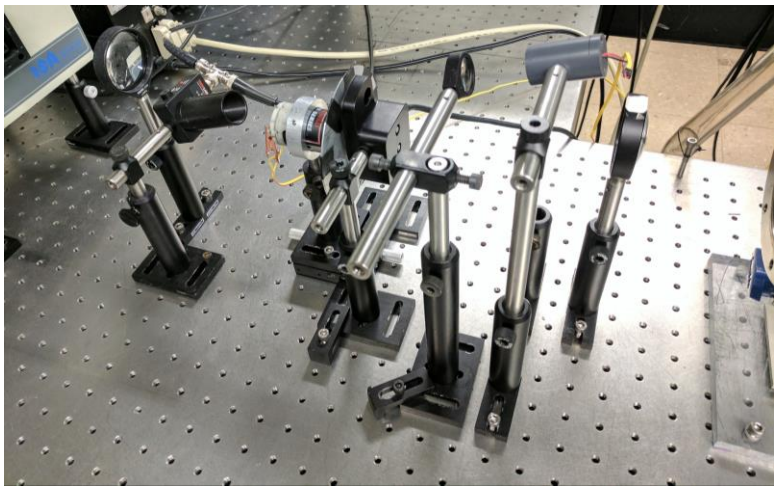

Figure 3.4: Near view of gating system for all cases of experimental setup

3.4. Experiments

A summary of experiments conducted in this study is listed in Table 3.1. Four sections of tests are covered with these 11 tests: 1) Various high explosives at low resolution in air (Tests 1-4), 2) Air vs. Nitrogen environment comparison of RDX at low resolution, 3) Higher resolution spectra of features indicated in first section of tests, and 4) Higher resolution spectra in air and nitrogen.

Timing was checked before each test with the procedure previously described. Charges were prepared prior to the tests by Professor Glumac. Detonators were placed inside a plastic sleeve for mounting and alignment purposes with small amount (~1-2 grams) of high explosive at the end of the detonators. Charges would be placed inside the blast chamber and then sealed. Air environment tests utilized the atmosphere. For the nitrogen environment tests the chambers would be vacuumed and re-pressurized to ~3 psi with nitrogen. This process was repeated four to five times before the tests.

Detonators were triggered using a custom fireset made by Professor Glumac consisting of a 1 μF capacitor charged to 5 kV and discharged across a triggered spark gap. Timing was monitored using an oscilloscope and fast photodiode to monitor first light with respect to the trigger signal.

Table 3.1: Experimental test matrix

Test #	Explosive/Detonator	Spectral Range (nm)	Resolution	Environment	Equipment Setup
1	RDX/RP1	880-1660	Low	Air	Case 1
2	Composition B/RP1	880-1660	Low	Air	Case 1
3	HMX/RP1	940-1580	Low	Air	Case 3
4	PETN/RP1	940-1580	Low	Air	Case 3
5	RDX/RP1	880-1660	Low	Nitrogen	Case 1
6	RDX/RP1	980-1070	High	Air	Case 2
7	RDX/RP1	1080-1170	High	Air	Case 2
8	RDX/RP1	1170-1250	High	Air	Case 2
9	RDX/RP1	1540-1620	High	Air	Case 2
10	RP80	990-1140	High	Air	Case 4
11	RP80	990-1140	High	Nitrogen	Case 4

3.5. Data processing

For each test a standard wavelength calibration and intensity calibration was performed. Several sources were used to check the accuracy of wavelength calibrations, but the final implemented calibrations used either argon or neon lamps as sources. An example of one such calibration is shown below. Figure 3.5 shows the raw spectrum from Test 6 with peak pixels labelled and Figure 3.6 shows the corresponding Ar I lines listed on NIST atomic spectra database [17]. A pixel to wavelength calibration was performed from the points in Figures 3.5 and 3.6 along with quadratic fit, which is shown in Figure 3.7 below. The fit shows good agreement with the chosen calibration.

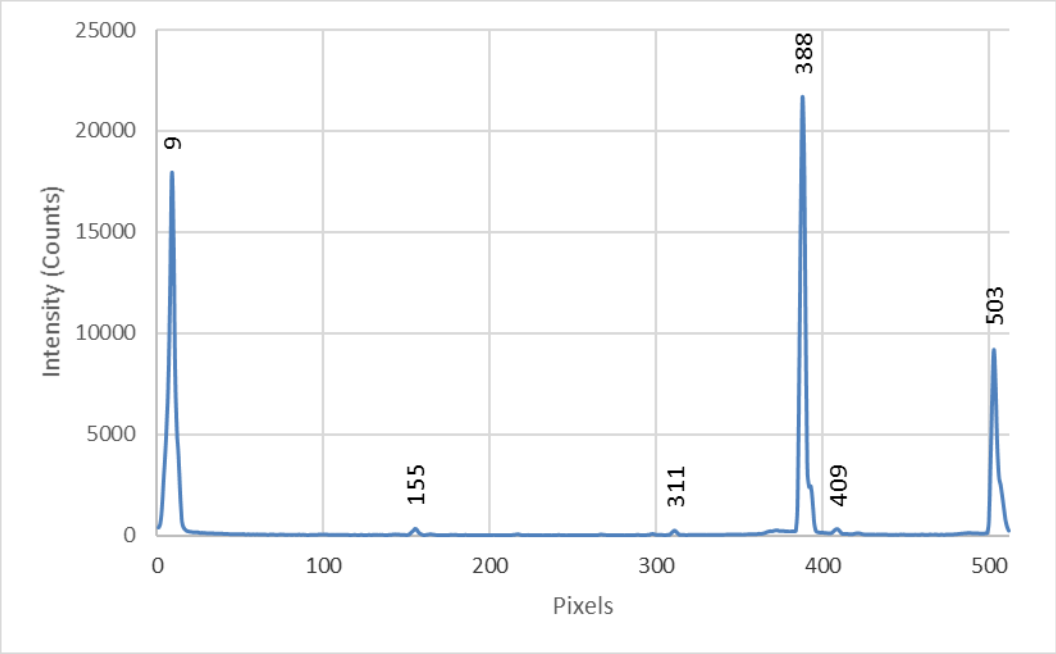

Figure 3.5: Test 6 Ar raw spectrum

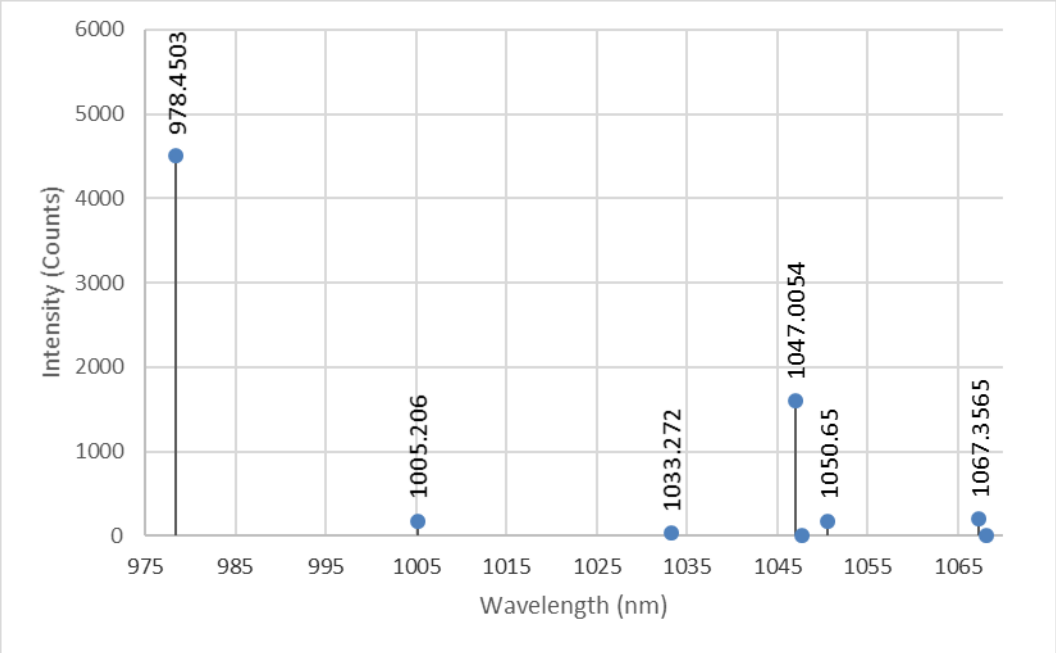

Figure 3.6: Test 6 Ar I lines from NIST atomic spectra database

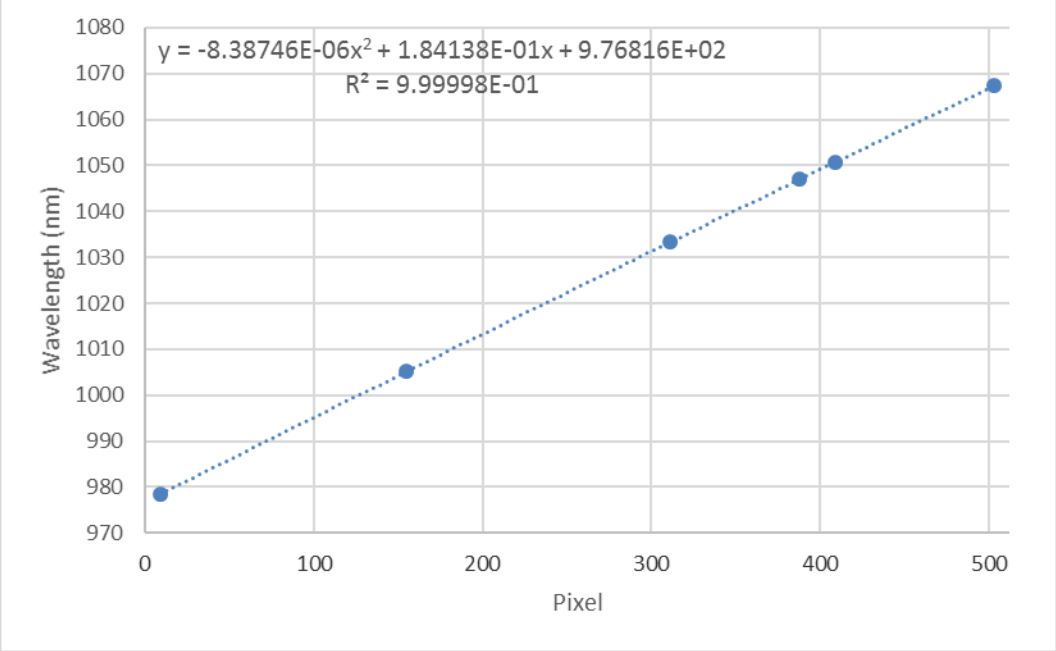

Figure 3.7: Test 6 pixel to wavelength calibration

For the intensity calibration either a CI Systems blackbody source (Model: SR-2-32-SA) heated to 1248 K or Newport 6319 quartz tungsten halogen lamp heated to 3200 K were used. Blackbody sources were placed at the focal point of the upstream lens and spectra was collected when the rotating disk was operating. Blackbody sources were estimated to follow Planck's law of black-body radiation shown in Equation 3.1 below.

$$\boldsymbol{I(\lambda, T) = \frac{2hc^2}{\lambda^5} \frac{1}{e^{\frac{hc}{\lambda kT}} - 1}} \qquad \text{Eq. 3.1}$$

An intensity correction ratio was determined by dividing the normalized calculated spectra by the normalized experimental blackbody spectra and then multiplying each test spectra by this ratio.

CHAPTER 4: RESULTS

4.1. Synopsis

All test spectra are compiled in Appendix A, and the results are summarized here in more concise plots for comparison. All noteworthy spectra from the tests listed in Table 3.1 are shown in Figures 4.1 – 4.4. Some atomic features appear with mostly bands or continuum emission prominent in most of the spectra. The center wavelengths of the most notable features are also listed in Table 4.1 below and will be discussed more in depth in the following chapter.

Table 4.1: Most notable features of experimental data

Test #	Center Wavelength of Notable Features (nm)
1	1015, 1035, 1125, 1222, 1563
2	1133, 1222, 1560
3	1184, 1225, 1537
4	1225, 1535
5	940, 1015, 1180, 1225, 1535
6	1037
7	1130
8	1180, 1200, 1222
9	N.A.
10	1119
11	1119

4.2. Various high explosives (Low resolution)

The four high explosives spectra that were tested in air in low resolution spectrometer systems are presented in Figure 4.1. The explosives include RDX, Composition B, HMX, and PETN and all were detonated using RP1 detonators. All four spectra show a common general trend, while the most prominent features are observed in Test 1 (RDX). The most common feature shared between Tests 1-4 is the feature centered approximately at 1222 nm. Test 1 and 2 show common features at approximately 1125 and 1560 nm. Test 3 and 4 appear to share common features at approximately 1185 and 1537 nm.

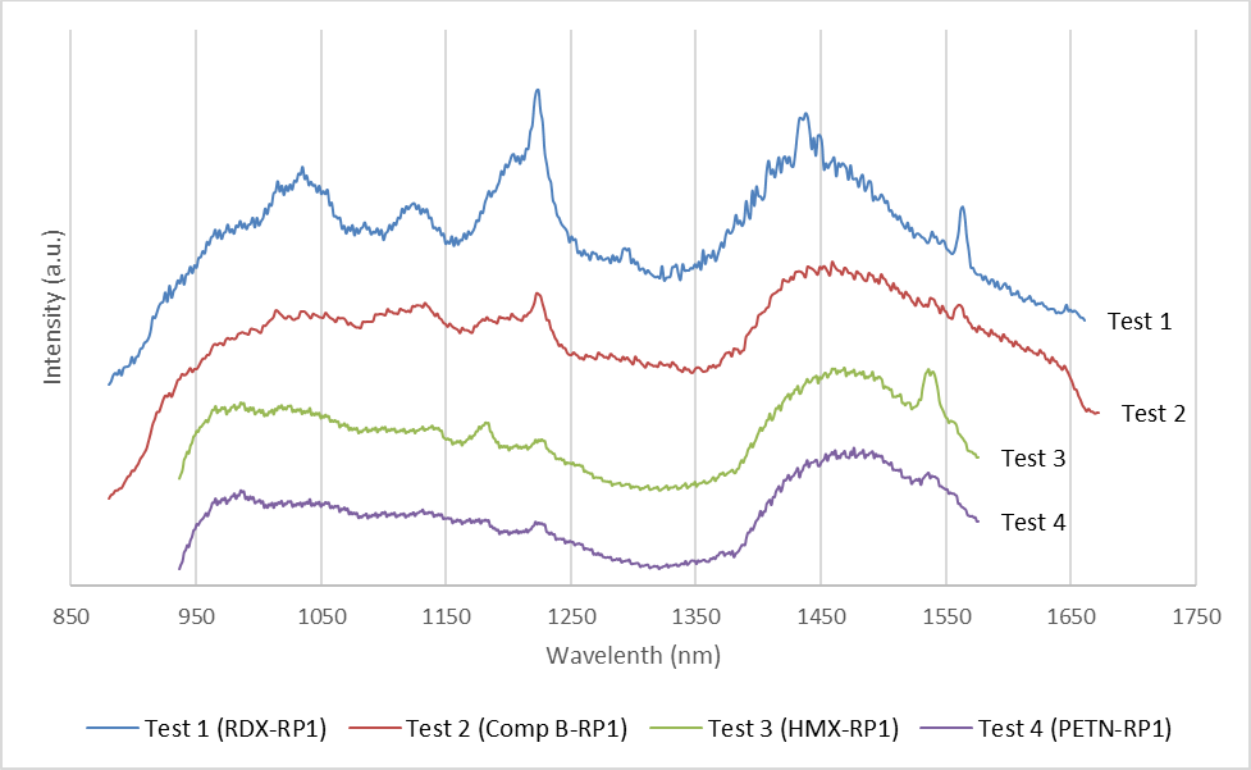

Figure 4.1: Various high explosives (Tests 1-4) low resolution spectra in air

4.3. RDX air vs. nitrogen environment (Low resolution)

Results from Test 1 and Test 5 are given in Figure 4.2 below. This plot shows a direct comparison of RDX low resolution spectra in an air and nitrogen environment. Both spectra once again show common features, but the Test 5 spectra show what appears to be several atomic lines not present in Test 1. The feature centered at 1222 nm observed in Tests 1-4 is still present in Test 5, but it is less distinguished.

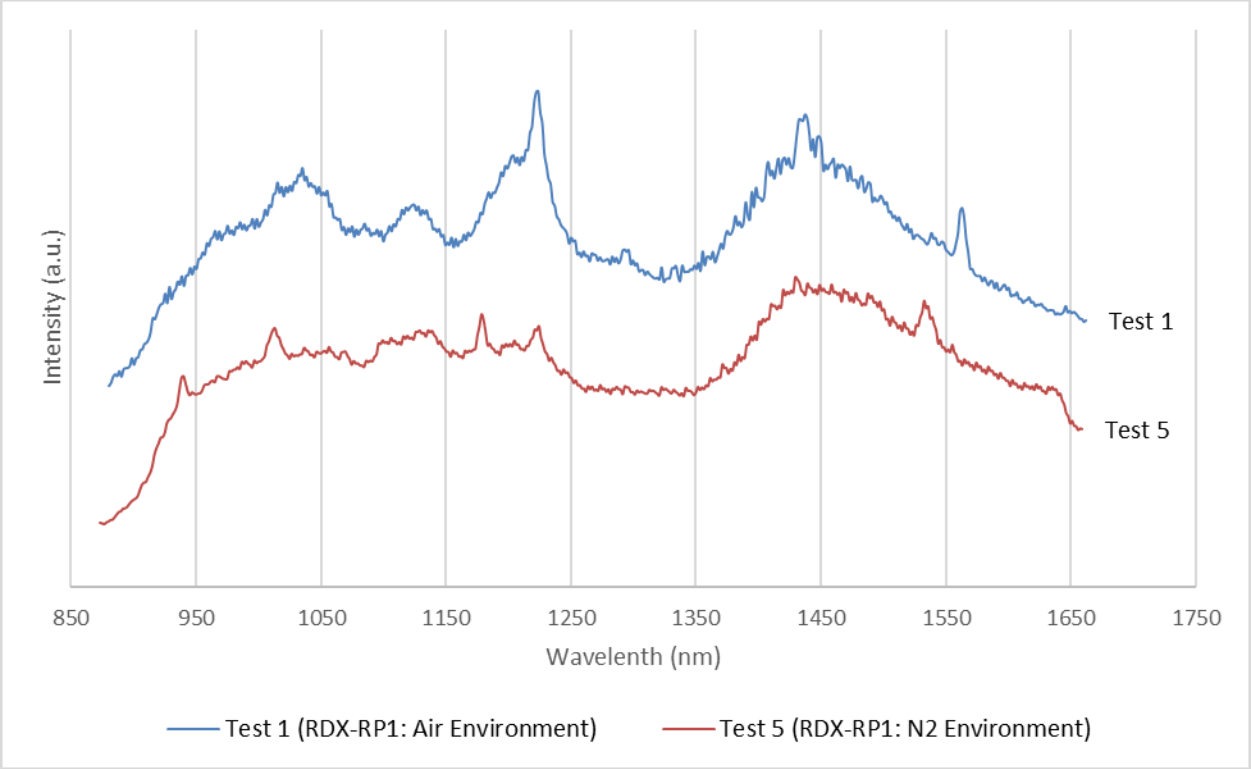

Figure 4.2: RDX low resolution spectra (Tests 1 and 5) in air and nitrogen environment

4.4. Notable features of RDX (High resolution)

Several key features from Test 1 were chosen to perform higher resolution tests. These features are included in Tests 6-9 that are featured in Figure 4.3. Test 9 was exempted from this plot because of failed replication of the feature seen from Test 1. Most of the higher resolution spectra match those features observed in Test 1. Only in Test 8 was there an additional feature not seen in Test 1. This feature appears to be an atomic line centered at approximately 1180 nm.

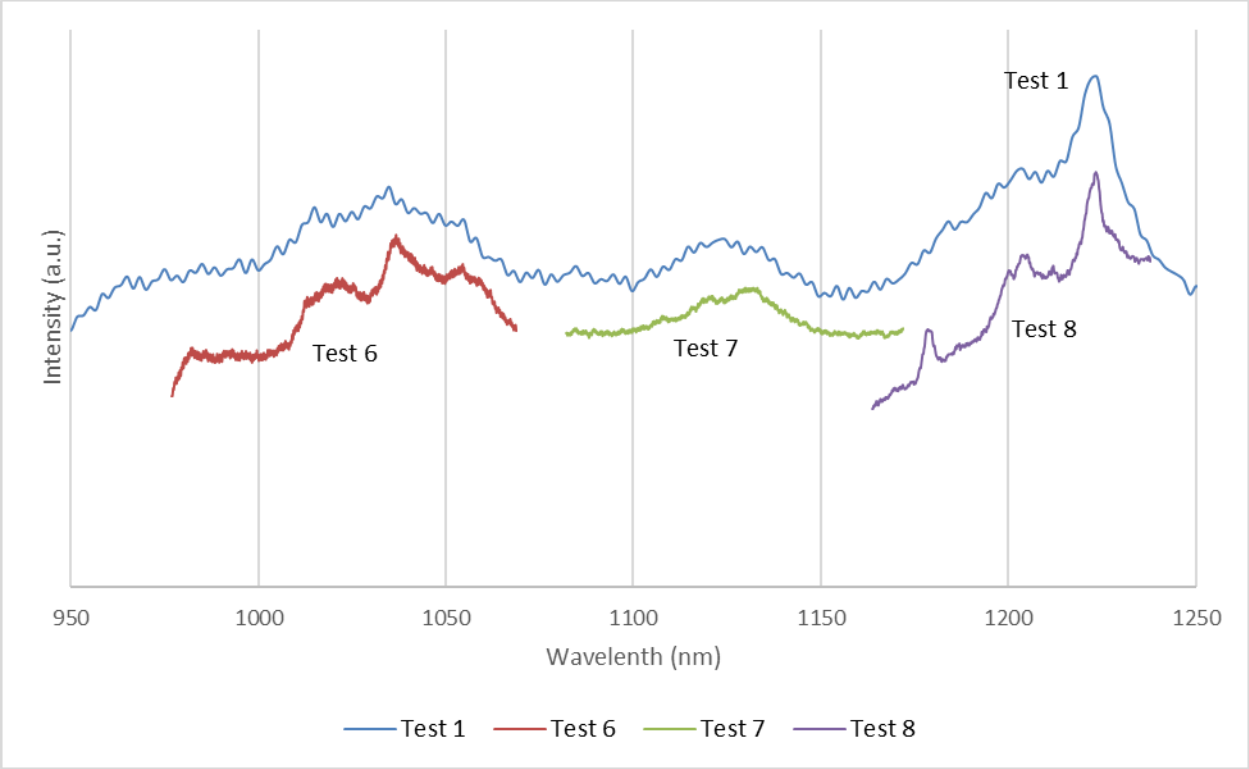

Figure 4.3: RDX low and high resolution spectra (Tests 1, 6-8) in air

4.5. Notable features of RDX air vs. nitrogen environment (High resolution)

Two smaller scaled tests excluding any explosive were conducted with RP80 detonators at higher resolution in air and nitrogen environment. These two spectra from Tests 10-11 are plotted in Figure 4.4. The results from Tests 10-11 do not share any notable features to similar Test 1 and 5. The only feature appears at approximately 1119 nm and it is seen in both Test 10 and 11.

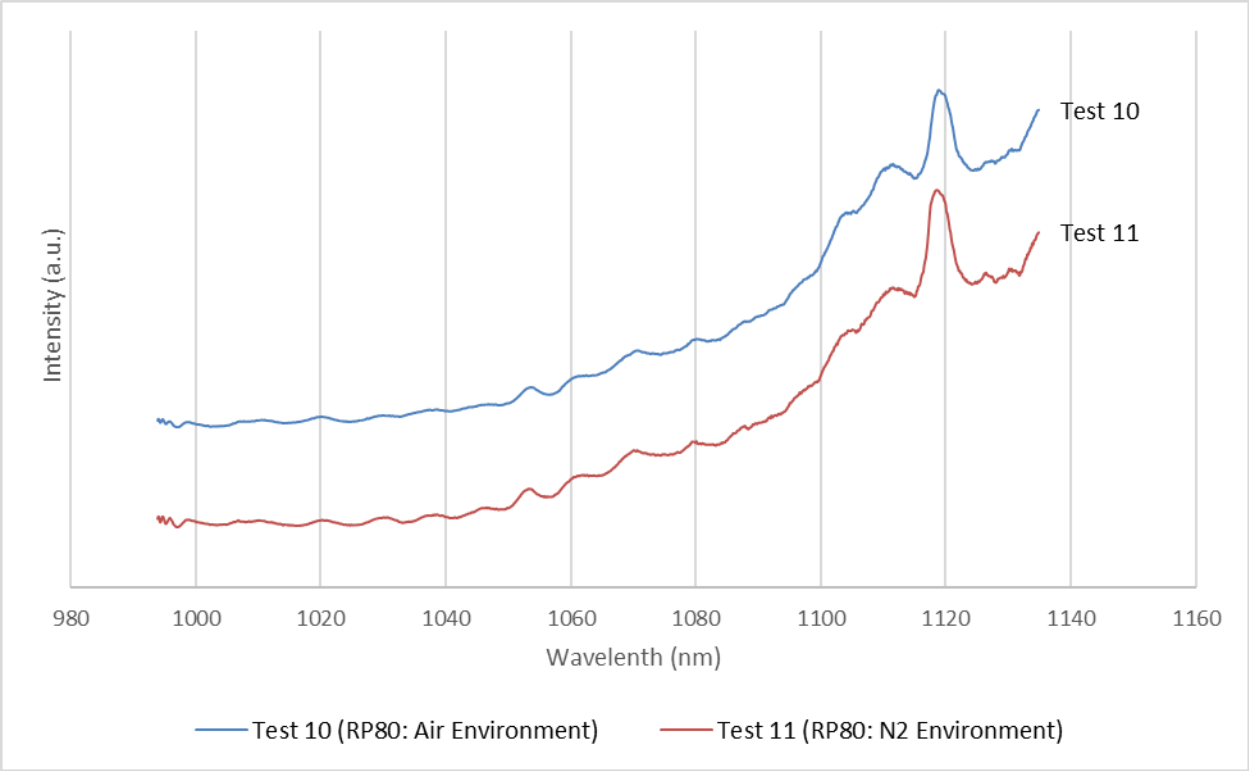

Figure 4.4: RP80 high resolution spectra (Tests 10-11) air vs. nitrogen environment

CHAPTER 5: DISCUSSION

5.1. Overview

The intent of this chapter is to identify as many of the notable features listed in Table 4.1 as possible. In these C/H/N/O systems, the most prevalent diatomics to consider are C2, CH, CN, CO, H2, N2, NH, NO, O2, and OH. Atomic sources such as neutral atoms of carbon, helium, nitrogen, and oxygen will be also considered, as well as metal impurities commonly found in explosive combustion, such as sodium, potassium, and calcium.

5.2. Discussion

As previously stated, all four spectra from Tests 1-4 show a common general feature at approximately 1220 nm that appears molecular in nature due to what appears to be possible vibrational levels degrading toward lower wavelengths. This feature was discussed through much of the near infrared shock research previously presented in Chapter 2 [4-10] and was observed in one high explosive emission study [15].

It appears the consensus thus far is that the feature around 1220 nm belongs to a collapsed Q-branch of the NO electronic band system, $C^2\Pi$ - $A^2\Sigma^+$. Some high-resolution spectra of this band were performed in a study by Amiot and Verges [17]. A spectroscopic simulation program called Specair [18] was used to simulate the best fit for the NO (C-A) electronic band and compare to the spectra from Test 1 and Test 8. These plots are shown in Figure 5.1 and Figure 5.2. The band head from the simulation appears to match quiet well with the spectra from Test 1 and Test 8. In

addition, comparison of the 1222 nm feature in air and nitrogen from Test 1 and 5 indicate a requirement for oxygen in the feature. From these results, the feature at 1220 nm appears to be belong to the electronic band of NO (C-A).

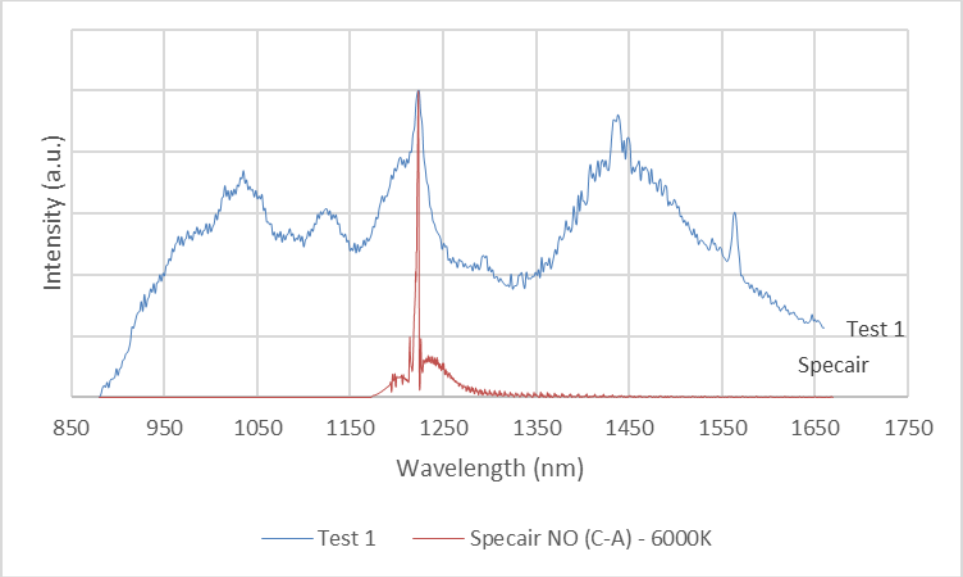

Figure 5.1: Specair simulation of NO (C-A) band compared with Test 1

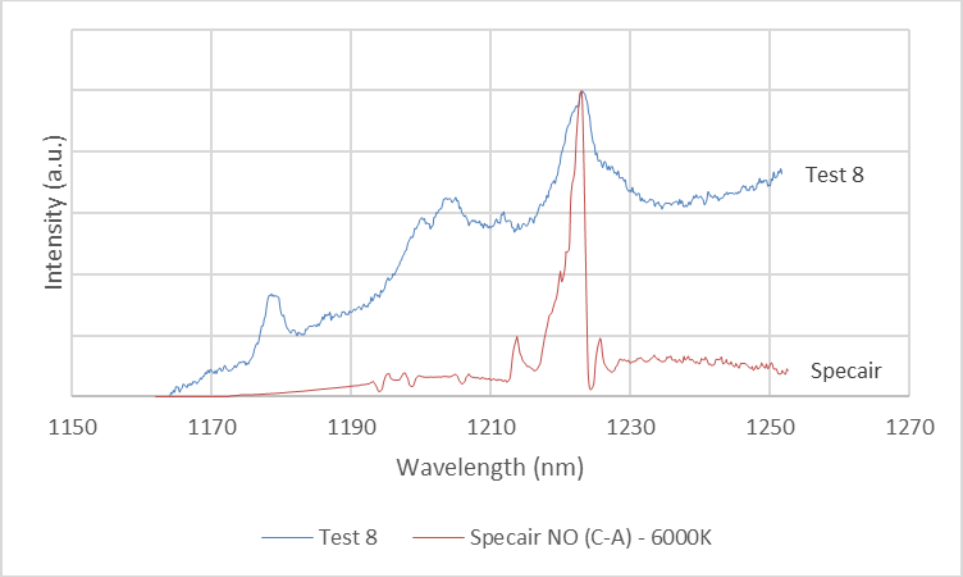

Figure 5.2: Specair simulation of NO (C-A) band compared with Test 8

Another feature prominent in Test 1 and slightly in Test 2 is centered at approximately 1035 nm. Once again, this feature is observed in previous near infrared shock work and time resolved high explosive emission research by Koch *et. al* [4-10,15]. This feature has been attributed to the N2 (+1) electronic band. Specair was used to simulate the best fit for the N2 (1+) electronic band and compare to the spectra from Test 1 and Test 6. These plots are shown in Figure 5.3 and Figure 5.4 below. The lower resolution of Test 1 matches well with the band head of the simulation, but when comparing with the higher resolution of Test 6, the fit is not the best. In addition, this feature was not observed in Test 5 with the nitrogen environment. This would suggest at the least that this feature requires oxygen present. So, at this point it is uncertain whether the feature at 1035 nm is due to the N2 (1+) electronic band.

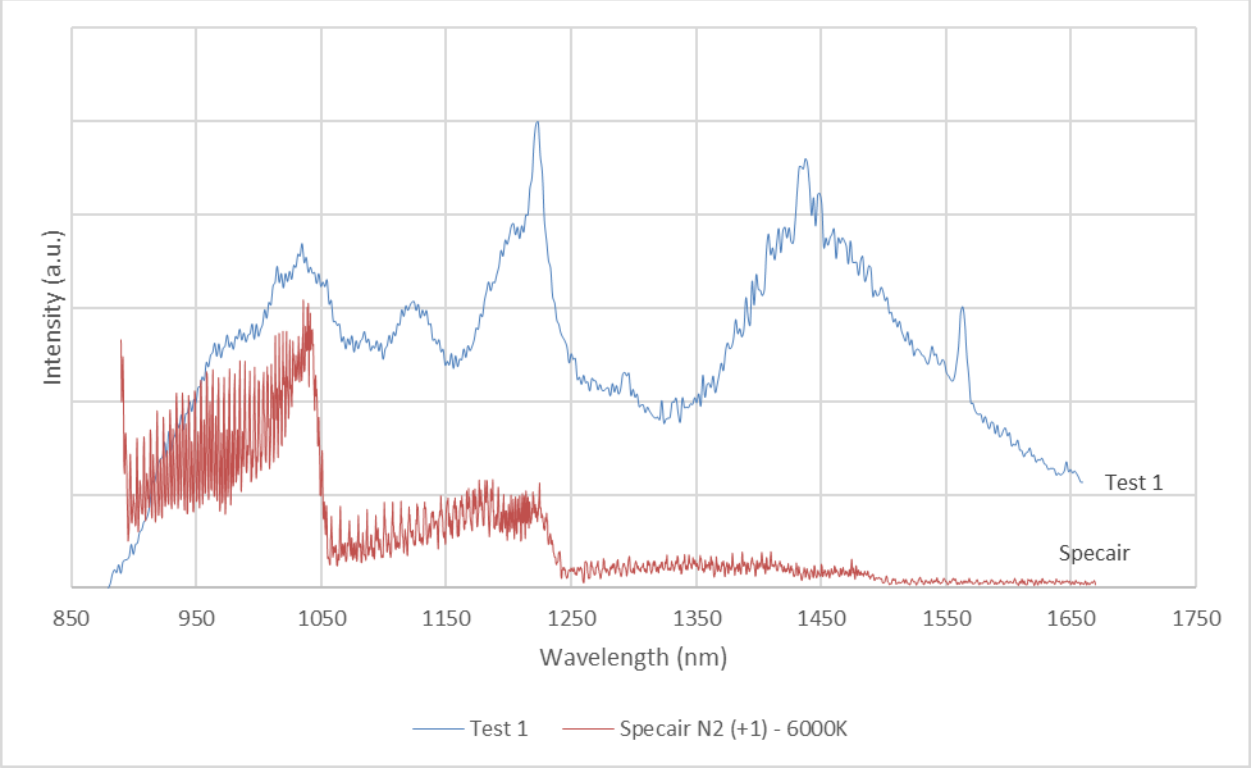

Figure 5.3: Specair simulation of N2 (1+) band compared with Test 1

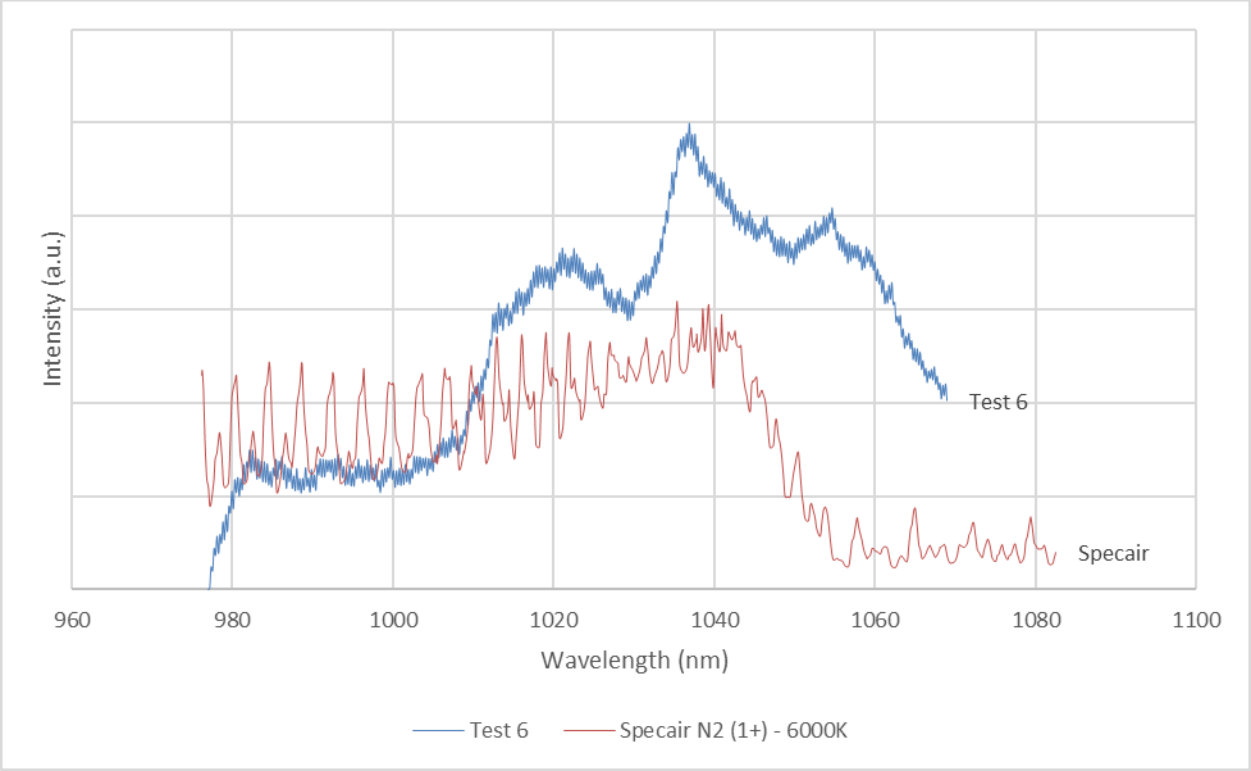

Figure 5.4: Specair simulation of N2 (1+) band compared with Test 6

The last prominent molecular feature of Test 1 is centered at approximately 1123 nm. This feature has not been extensively mentioned in previous studies, but it is clearly seen in spectra taken by Koch *et. al* [15]. The higher resolution spectra from Test 7 does not shed much clarity on the feature either. There appear to be several possible sources for feature. Using Specair again, the location of one such band head CN (Red) that could be a contributing factor to this structure is simulated in Figure 5.5. At this time the feature remains unidentified.

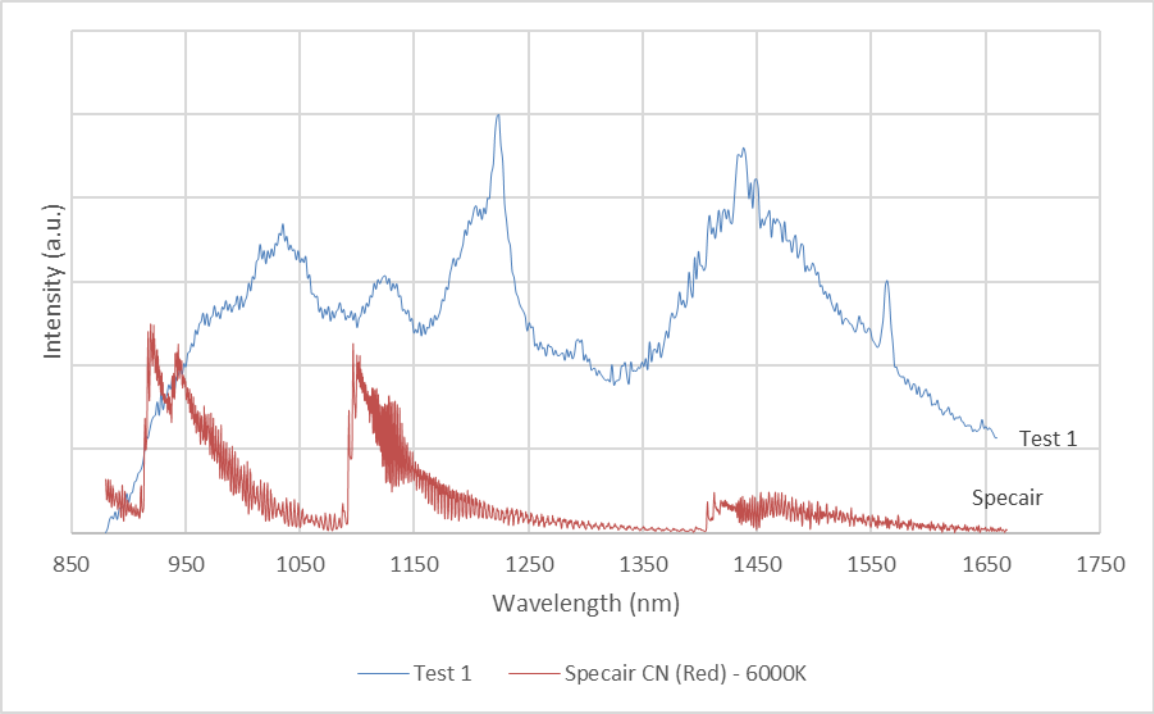

Figure 5.5: Specair simulation of CN (Red) band compared with Test 1

Most of the other features observed in this study appear to be atomic lines. Such features are prominent in Test 1, 2, 5, 8, 10, and 11. Features centered at 940 nm and 1013 observed in Test 5 appear to be N I lines [9,19]. Specair was used to simulate atomic nitrogen lines, shown in Figure 5.7, and the simulation shows good agreement with the experimental spectrum [18]. The feature at 1179 nm was identified as potassium impurity by Koch *et. al* [15, 19]. The feature is also located near a possible atomic carbon line, shown in Figure 5.8 [18]. Similarly, the features at 1535 nm and 1563 nm could also belong to nitrogen or carbon [19]. A summary of the possible identification of those observed features are shown in Table 5.1.

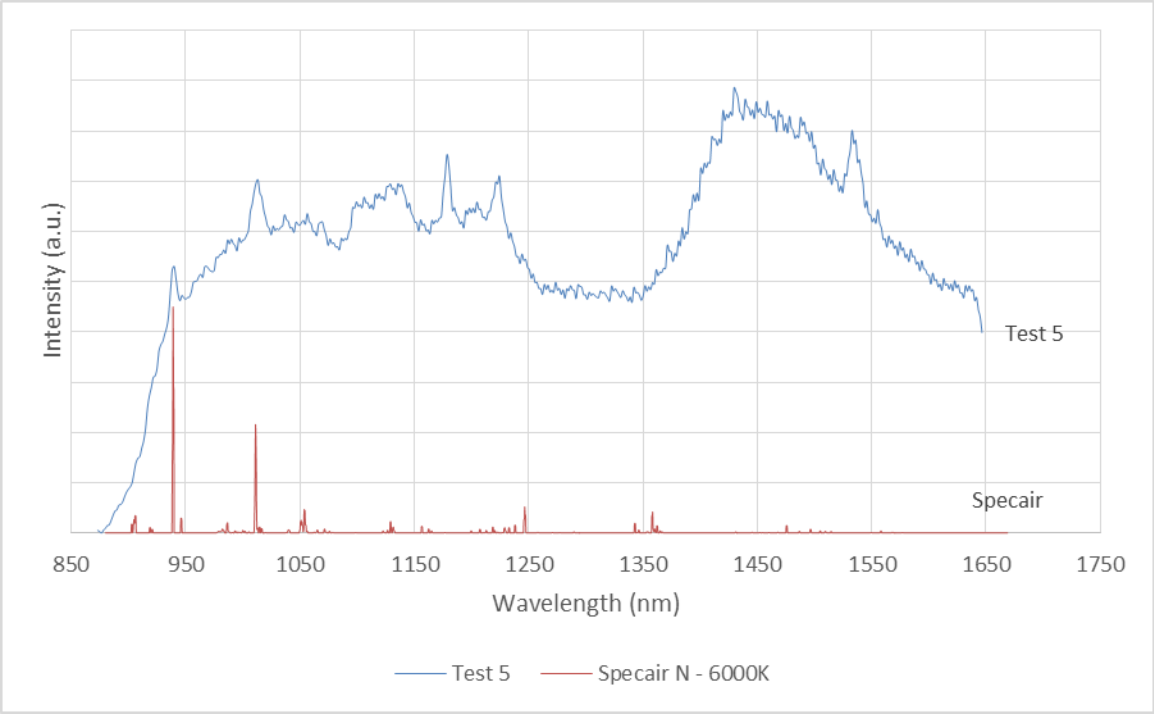

Figure 5.6: Specair simulation of atomic N I lines compared with Test 5

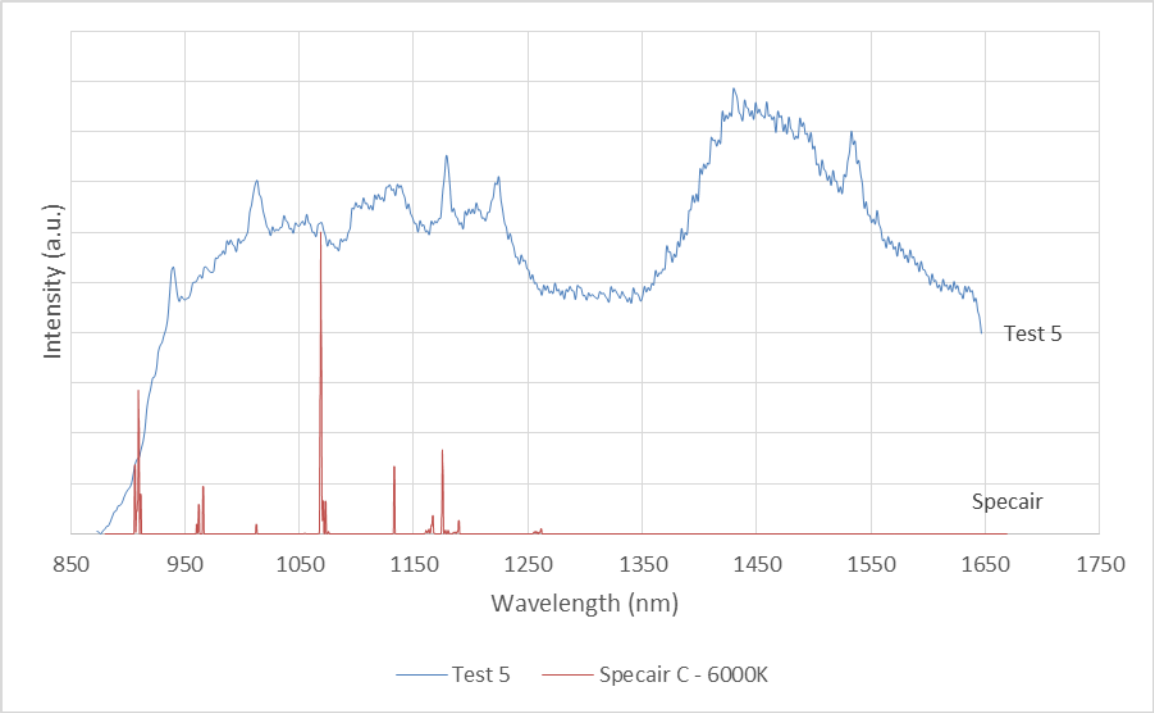

Figure 5.7: Specair simulation of atomic C I lines compared with Test 5

Table 5.1: Identification of notable spectra from tests results

Center Wavelength of Notable Features (nm)	Seen in Test #	Identification
940	5	N I
1013	1, 5	N I
1035	1, 6,	Possibly N2 (1+)
1123	1, 2, 7, 10, 11	Unidentified
1179	3, 5, 8	Possibly K I or C I
1222	1, 2, 3, 4, 5, 8	NO (C-A)
1535	3, 4, 5	Possibly N I or C I
1563	1, 2	Possibly N I or C I

CHAPTER 6: CONCLUSION

6.1. Summary and Conclusions

The aim of this research was to explore the early time breakout in the near infrared spectrum of various high explosives. Explosives tested include RDX, Composition B, HMX, and PETN, along with RP1 and RP80 detonators. A comparison of both low and high resolution tests was conducted in air and nitrogen environments resulting in a total of eleven tests. Notable spectral features were compared to previous studies conducted and emission spectrum of likely diatomic and atomic sources were investigated. This work introduced possibly some of the first work in early time-resolved emission spectroscopic measurements for several high explosive detonations in air and nitrogen. Some of the spectroscopic features and emitters appear to be positively identified, such as the prominent NO band at 1222 nm and several atomic nitrogen lines, while others still remain unknown. These features are due to short-lived species, that only occur at the microsecond time scale, at the onset of detonation.

6.2. Recommended Future Studies

This exploratory work should simply be considered as the beginning for future studies. But there are several key aspects that should be further studied. First, replicated tests under similar conditions should be performed to check repeatability of these results. If similar results are replicated to those found, then pursuit in identifying the key features of spectra left unidentified to should be a key goal. If different results are found then an explanation for any differences should be attempted.

As previously stated this study is limited to covering the range of 880 – 1660 nm with a resolution of approximately 3-4 nm and 0.5 nm. In addition, only the first 20 microseconds after the detonation was recorded. Future work should also include examine increased wavelengths into the mid infrared as well as higher resolution spectrum of the current study. This would assist in the identification and confirmation of the features observed here.

Further time resolved studies should also be implemented to allow a clearer understanding of how these spectrum progress. Once these features are identified then additional studies should be conducted, including but not limited to temperature, concentration, and identification diagnostics.

REFERENCES

[1] Fordham, Stanley. *High explosives and propellants*. 2nd ed. Oxford: Robert Maxwell, M.C., 1980.

[2] Agrawal, Jai Prakash. *High energy materials: propellants, explosives and pyrotechnics*. Weinheim: Wiley-VCH, 2011.

[3] Cook, Melvin A. *The science of high explosives*. Malabar: R.E. Krieger, 1971.

[4] Wurster, Walter H., Charles E. Treanor, and Herbert M. Thompson. "Nitric Oxide Bands near 1 μ in Shock-Heated Air." *The Journal of Chemical Physics* 37.11 (1962): 2560-563.

[5] Wurster, Walter H. "Quantitative spectroscopic studies with the shock tube." *Journal of Quantitative Spectroscopy and Radiative Transfer* 3.4 (1963): 355-64.

[6] Wray, Kurt L., Thomas J. Connolly. " Nitrogen and air radiation in the near IR." *Journal of Quantitative Spectroscopy & Radiative Transfer* 5 (1965): 111-23.

[7] Wurster, Walter H., and Paul V. Marrone. "Nitric oxide radiation in the near I.R. spectrum of shock-heated air." *Journal of Quantitative Spectroscopy and Radiative Transfer* 7.4 (1967): 591-604.

[8] Wurster, W. H., and P. V. Marrone. *Further Measurements of the Near IR Spectrum of Shock-Heated Air*. Technical Report. 1966.

[9] Wray, K. L. "Oscillator strengths of transitions between Rydberg states of nitric oxide in the near IR." *Journal of Quantitative Spectroscopy and Radiative Transfer* 9.2 (1969): 255-276.

[10] Benesch, W. M., and K. A. Saum. "Electric discharges in air: Near infrared emission spectrum." *Journal of Quantitative Spectroscopy and Radiative Transfer* 12.7 (1972): 1129-137.

[11] Weiser, Volker, and Norbert Eisenreich. "Fast Emission Spectroscopy for a Better Understanding of Pyrotechnic Combustion Behavior." *Propellants, Explosives, Pyrotechnics* 30.1 (2005): 67-78.

[12] Carney, Joel R., J. Scott Miller, Jared C. Gump, and G. I. Pangilinan. "Time-resolved optical measurements of the post-detonation combustion of aluminized explosives." *Review of Scientific Instruments* 77.6 (2006).

[13] Lewis, W. K., and C. G. Rumchik. "Measurement of apparent temperature in post-detonation fireballs using atomic emission spectroscopy." *Journal of Applied Physics* 105.5 (2009).

[14] Lewis, W. K., C. G. Rumchik, P. B. Broughton, and C. M. Lindsay. "Time-resolved spectroscopic studies of aluminized explosives: Chemical dynamics and apparent temperatures." *Journal of Applied Physics* 111.1 (2012).

[15] Koch, Jon D., Scott Piecuch, James M. Lightstone, Joel R. Carney, and Joe Hooper. "Time-resolved measurements of near infrared emission spectra from explosions: Pure pentaerythritol tetranitrate and its mixtures containing silver and aluminum particles." *Journal of Applied Physics* 108.3 (2010).

[16] Glumac, N. "Early time spectroscopic measurements during high-explosive detonation breakout into air." Shock Waves 23.2 (2012): 131-38.

[17] Amiot, C., and J. Verges. "Fine Structure of the C 2 Π- A 2 Σ and D 2 Σ - A 2 Σ Band Systems of the NO Molecule: Homogeneous and Heterogeneous Perturbations." *Physica Scripta* 25.2 (1982): 302-11.

[18] *Specair*. Computer software. Vers. 3.0. SpectralFit S.A.S.

[19] "NIST: Atomic Spectra Database Lines Form." *NIST: Atomic Spectra Database Lines Form*.

APPENDIX A: TEST SPECTRA

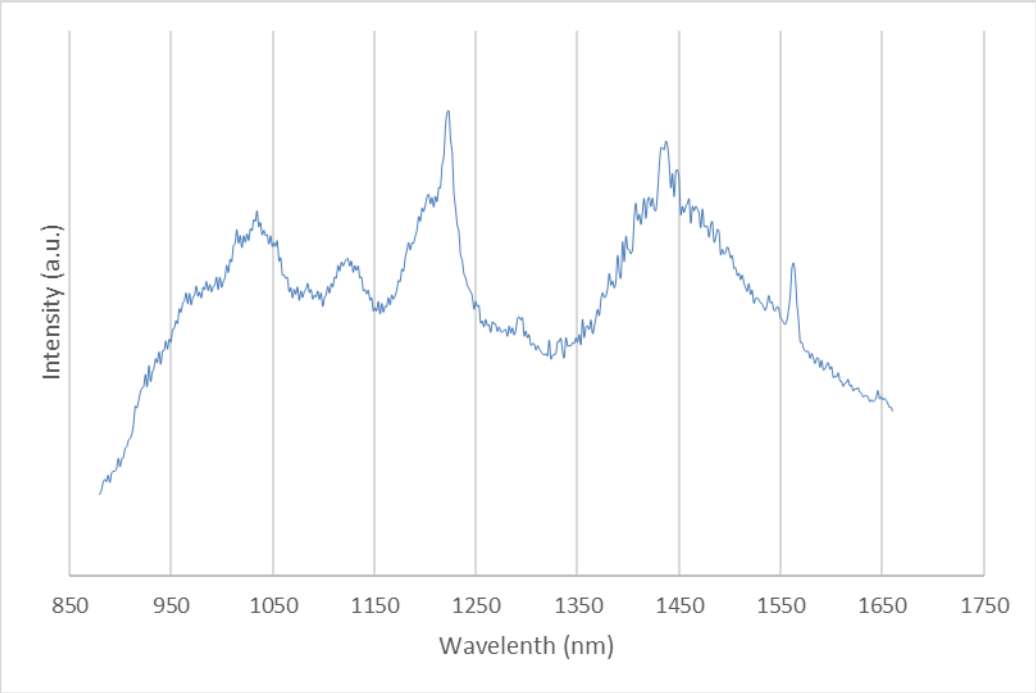

Figure A.1: Intensity calibrated Test 1 spectra

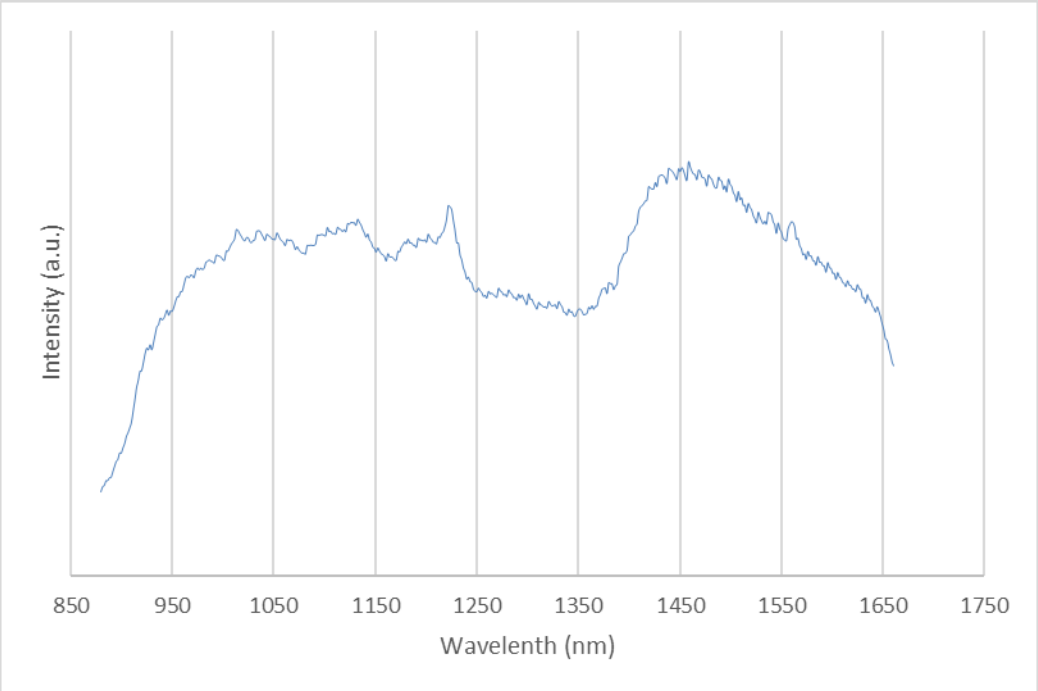

Figure A.2: Intensity calibrated Test 2 spectra

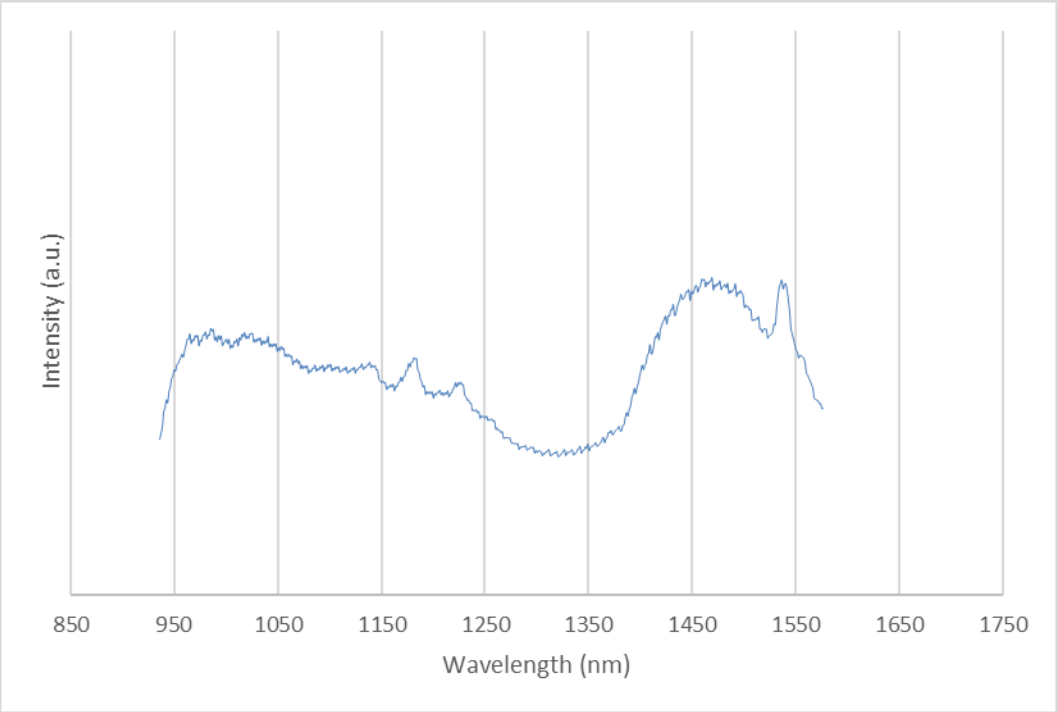

Figure A.3: Intensity calibrated Test 3 spectra

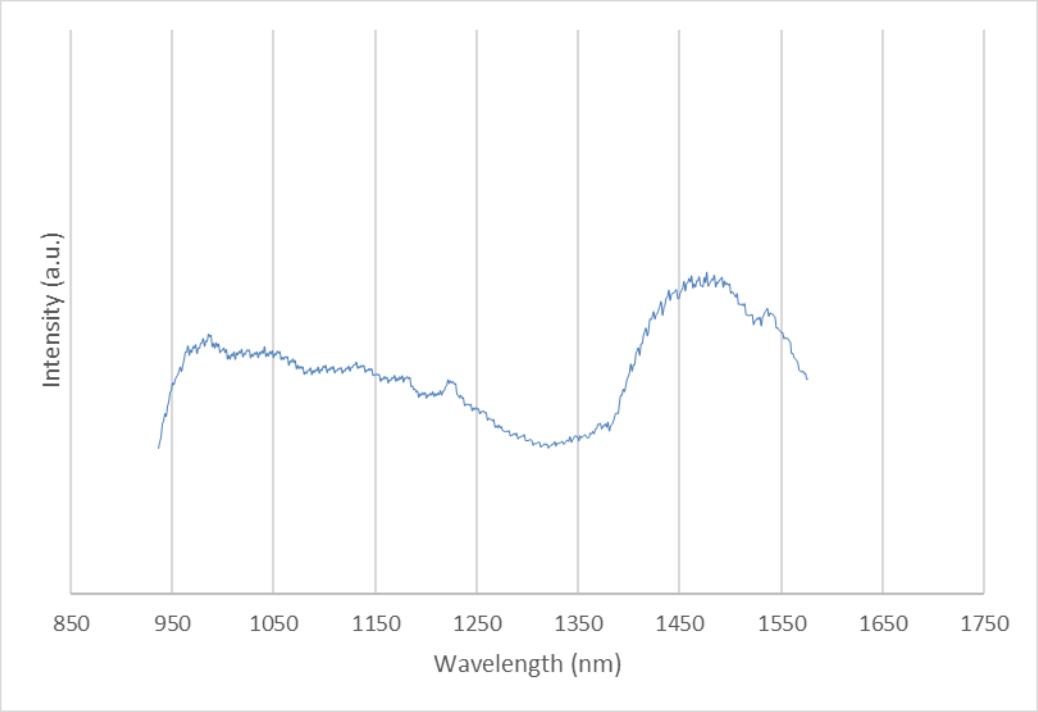

Figure A.4: Intensity calibrated Test 4 spectra

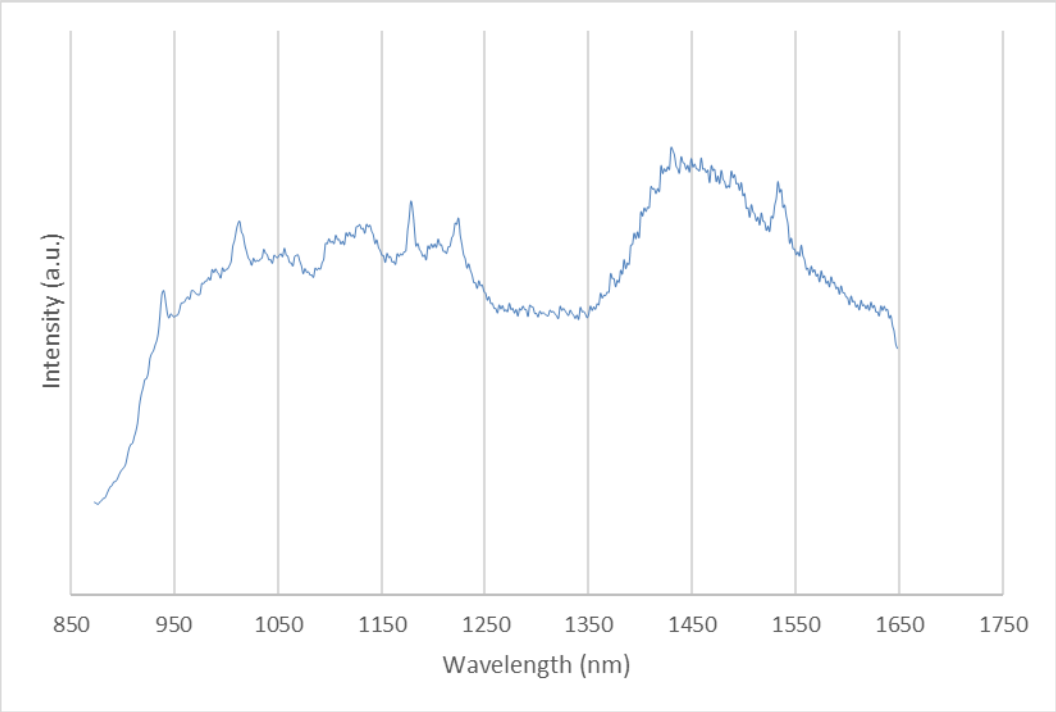

Figure A.5: Intensity calibrated Test 5 spectra

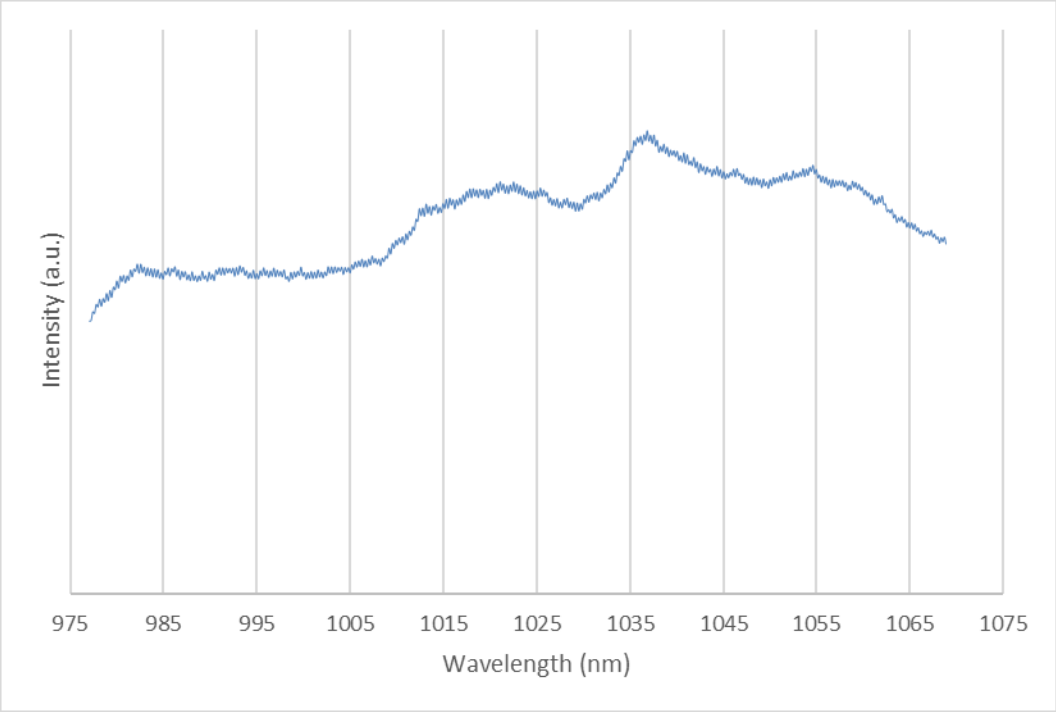

Figure A.6: Intensity calibrated Test 6 spectra

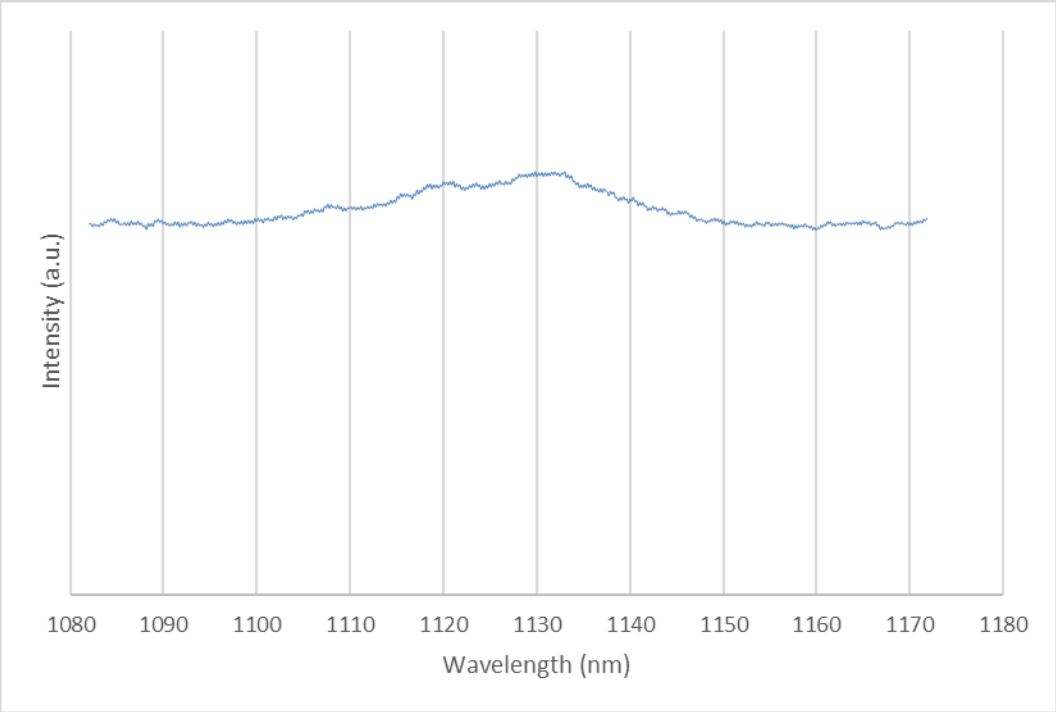

Figure A.7: Intensity calibrated Test 7 spectra

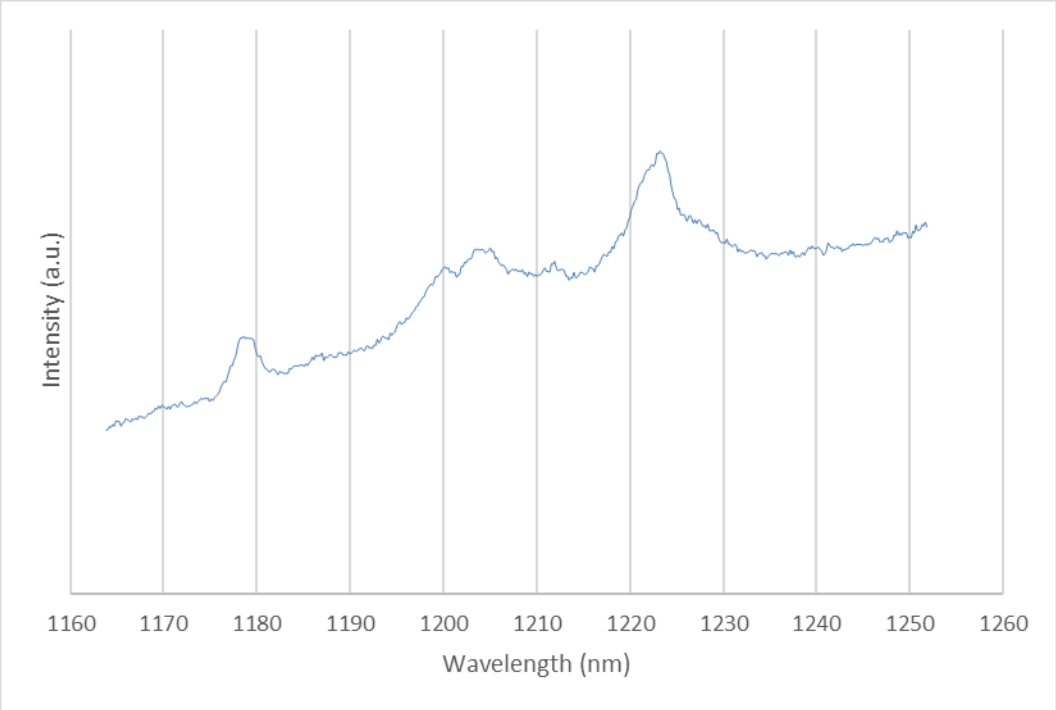

Figure A.8: Intensity calibrated Test 8 spectra

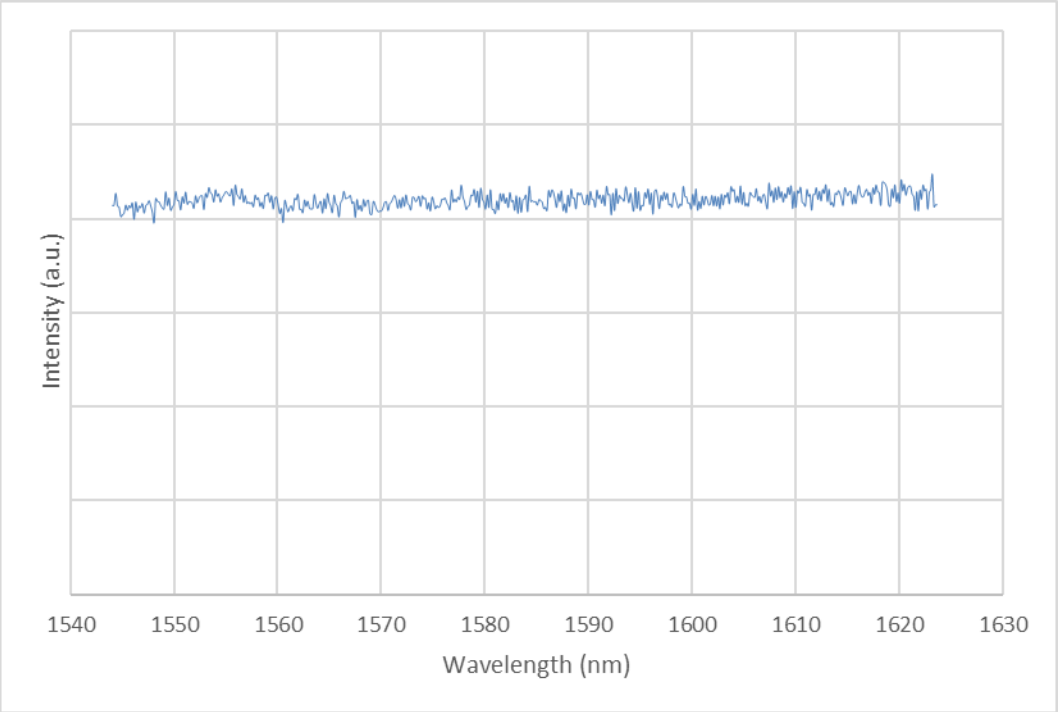

Figure A.9: Intensity calibrated Test 9 spectra

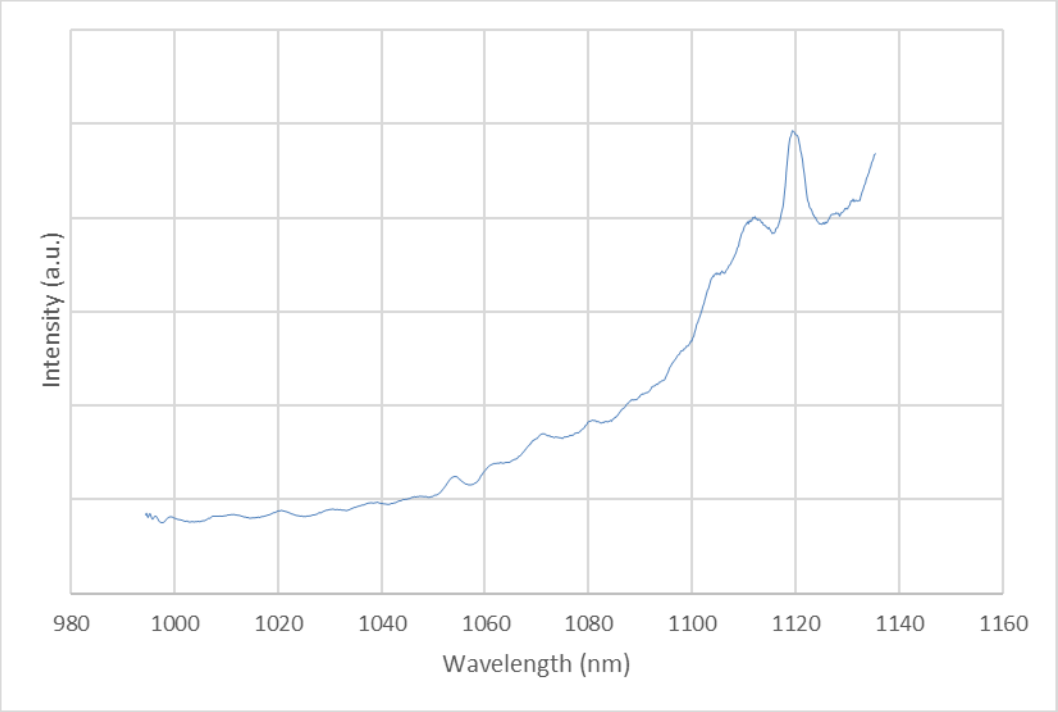

Figure A.10: Intensity calibrated Test 10 spectra

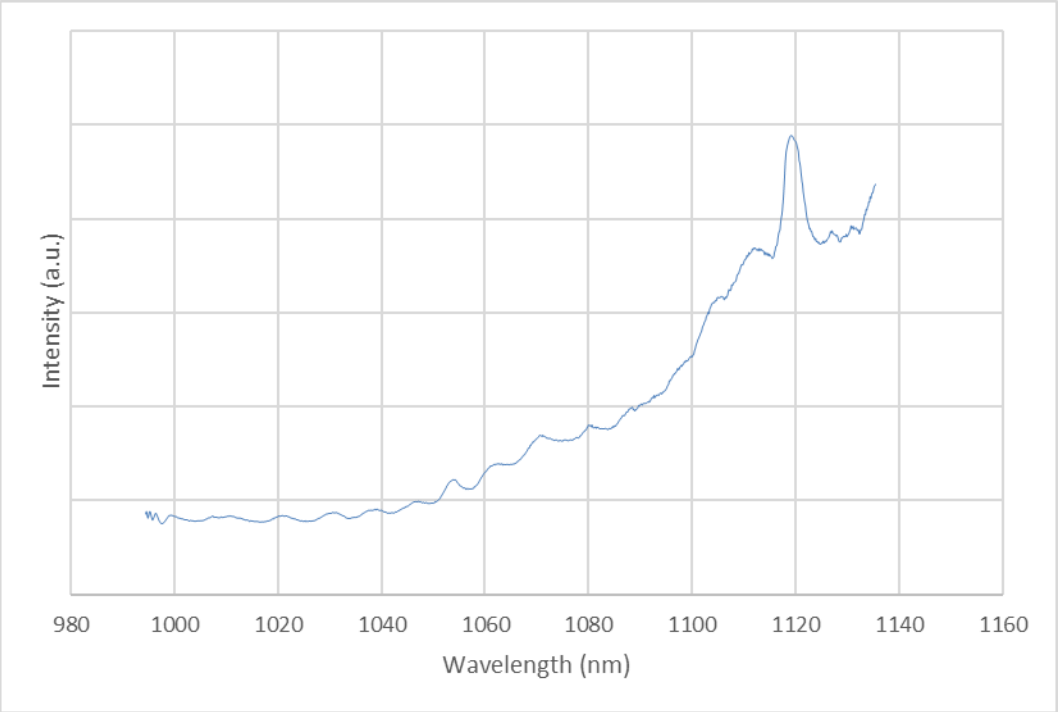

Figure A.11: Intensity calibrated Test 11 spectra